RESEARCH

Structural Performance of Ferrocement Beams Incorporating Longitudinal Hole Filled with Lightweight Concrete

Yousry B. Shaheen[1], Boshra A. Eltaly[1], Shaimaa G. Yousef[1] and Sabry Fayed[2*]

Abstract

In this study, 10 ferroconcrete concrete (FC) beams with lightweight cores reinforced with welded steel mesh as a shear reinforcement were evaluated under three-point bending tests along with two conventionally normal-weight concrete (NWC) beams. Expanded polystyrene and lightweight aerated autoclaved brick wastes were used to create lightweight core concrete. The main factors include the type of lightweight concrete used for the core, beam concrete type, the form and number of holes, the existing steel mesh fabric, the hollow, and the hole placement. This study was done on the tested beams' ductility index, failure modes, first cracking loads and associated deflections, and ultimate loads besides corresponding deflections. Experimental results showed that the use of FC, various filling materials, and welded steel meshes in place of traditional stirrups enhanced the ultimate load by 36.6–107.3%, the ultimate deflection by 6–272%, and the ductility by 89–1155% when referenced to a control NWC beam. When the holing ratio increased from 10 to 20%, the ductility of FC beams was enhanced by 307.7%. Proposed equations were developed to predict the ultimate load and bending moment capacity of FC beams while taking into account the compressive strength of the beam body and filling material, the holing ratio, the tensile reinforcement ratio, and the volume fraction of the steel mesh.

Highlights

- This study is focusing on structural performance of ferrocement beams with lightweight cores reinforced with steel mesh fabric as a shear reinforcement.
- Lightweight core concrete with steel mesh fabric reinforcement was made either using lightweight aerated autoclaved brick aggregate (LAABA) or expanded polystyrene (EP).
- Impact of core lightweight concrete type, shape/number of holes, existing steel mesh fabric, concrete type, existing hollow core, positioning of hole on structural performance of the beams were performed.
- Structural performance factors such ductility index, failure mechanism, first cracking loads and deflections and ultimate loads and deflections were studied.

Keywords Ferrocement beams, Lightweight concrete, Normal concrete beams, Welded wire mesh, Core material types, Longitudinal hollow core, Capacity, Cracks, Ductility, Deflection, Flexural, Shear behavior

*Correspondence:
Sabry Fayed
sabry_fayed@eng.kfs.edu.eg; sabrielmorsi@yahoo.com

[1] Department of Civil Engineering, Menoufia University, Shebin ElKoum, Egypt
[2] Civil Engineering Department, Faculty of Engineering, Kafr El-Sheikh University, Kafr El-Shaikh 33511, Egypt

Shaheen *et al. Int J Concr Struct Mater*   (2023) 17:21

Page 2 of 24

1 Introduction

For the construction of multi-story buildings, hollow-core flexure members (beams and slabs) are essential because they have advantages over conventional solid specimens, including faster construction, long-span beams, maintaining a good ratio of beam and slab strength, passing air conditioning and electrical services, and increasing the clear height of the story. They also have lower self-weight, which reduces dead loads and lowers total cost. Additionally, eliminating concrete used for structural members aids in sustainability by preserving the environment through lower resource use, lower carbon dioxide (CO_2) emissions, and lower embodied energy. Using longitudinal voids in reinforced concrete (RC) beams is one of the methods to reduce the concrete from the tension zone to get lightweight beams. Al-Maliki et al. (Al-Maliki et al., 2021) investigated the effect of the hollow ratio, which ranged from 7 to 14%, on the structural performance of conventional normal-weight RC beams. The final load was found to have decreased by between 37.14 and 58.33%, but the deflection had improved noticeably. Recent years have seen the presentation of numerous studies (Abbass et al., 2020; Alnuaimi et al., 2008; Dhinesh & Satheesh, 2017; Hassan et al., 2018; Kumbhar & Jadhav, 2018; Parthiban & Neelamegam, 2017; Varghese & Joy, 2016) examining the structural behavior of hollow-core beams. The findings demonstrated that rectangular hollow (Alnuaimi et al., 2008; Dhinesh & Satheesh, 2017; Kumbhar & Jadhav, 2018; Parthiban & Neelamegam, 2017), circular hollow (Hassan et al., 2018; Varghese & Joy, 2016), and square hollow (Abbass et al., 2020) increased deflections while reducing ultimate load. The outcomes also showed that 0.53 was the ideal ratio between the depth of the circular hollow-core center and the beam (Hassan et al., 2018; Varghese & Joy, 2016). Also, the results show that the hole shape and size up to half the beam width does not affect the failure mode compared to the solid control beam (Abdulhusain & Ismael, 2020; Al-Smadi, 2022).

When compared to conventional reinforced concrete, ferrocement is a building material that has excelled in testing for crack control, impact resistance, and toughness because of the homogeneous distribution of fiber reinforcement within the material and the close spacing of those fibers. One of ferrocement's key benefits is that it can be built with a variety of characteristics, attributes, and prices depending on the needs and budget of the customer. Ferrocement is a type of thin-walled reinforced concrete that is often made of hydraulic cement mortar reinforced with layers of continuous wire mesh that are quite small in size and tightly spaced (ACI Committee, 1997; ACI Committee, 1988; Manikandan et al., 2015). The facts that ferrocement components are readily available in the majority of nations, that no skilled labor is needed, and that it can be built using both prefabrication and do-it-yourself methods make ferrocement one of the most affordable and alluring alternatives to traditional methods for concrete structures strengthening. Water tanks, roofs, boats, pipes, silos constructions, and affordable housing are some conventional ferrocement applications (Arif & Pankaj 1999; Naaman & Al-Shannag, 1994; Naaman, 2000a; Shah et al., 1984). Additionally, ferrocement has a variety of uses, including precast ferrocement pieces, retaining walls, sculptures, bus shelters, bridge decks, repair work, and various roofing systems (Aboul-Anen et al., 2009; Al-Kubaisy & Jumaat, 2000; Wang et al., 2004). Numerous researchers have documented the benefits of ferrocement when compared to traditional RC. The quality requirements for the design and maintenance of structural parts can also be defined using a variety of test data (Elavenil & Chandrasekar, 2007; Fahmy et al., 2014; Shaaban et al., 2018; Shaheen et al., 2014). According to these investigations, ferrocement has advantages, including simple prefabrication and affordable maintenance and repair. The entire test data on the tensile behavior of 12.5-mm–thick ferrocement plates were examined. The findings demonstrated that extremely satisfactory predictions could be made for the composite parameters of elastic modulus and ultimate tensile strength. The findings demonstrated that, in comparison to beams reinforced with non-metallic mesh, those reinforced with metal wire mesh indicated better cracking patterns (Elavenil & Chandrasekar, 2007). Moreover, the effect of filling material type on hollow-core beams was investigated (Shaheen et al., 2014). The results proved that the first cracking, serviceability and ultimate loads, stiffness, and the energy dissipation capacity are all slightly influenced by the type of core filling. Additionally, the performance of lightweight ferrocement beams reinforced with steel meshes was investigated (Fahmy et al., 2014; Shaaban et al., 2018). The findings demonstrated that the ferrocement beams have an increased elasticity index compared to the conventional beams. El-Wafa et al. (Shaaban et al., 2018) demonstrated that ferrocement beams outperformed RC beams in terms of performance and achieved more cracks. The welded wire mesh enhanced the flexural and shear performance of the sandwich beams in another investigation (El-Wafa & Fukuzawa, 2010). According to Shaheen et al. (Chakrawarthi et al., 2022), adding more layers of welded and expanded steel mesh to ferrocement composites delays the onset of the first cracking. The improvement of structural behavior, particularly bending features, is greatly aided by the employment of these meshes as a reinforcement in the ferrocement thin composites. When compared to traditional RC members, the findings of various

investigations indicated that ferrocement composites had higher ultimate and serviceability loads, fracture resistance management, high ductility, and strong energy dissipation capabilities (Baraghith et al., 2022; Basha et al., 2020; Fayed, 2019; Mansour & Fayed, 2021; Shaheen & Eltehawy, 2017; Shaheen et al., 2018, 2020a, 2020b, 2022).

Ferrocement is a unique material composed of cement mortar and reinforcement in the form of tightly spaced wire mesh either metallic or non-metallic type. Since no coarse aggregate is utilized, the ferrocement components can be built in any new shape, and the meshes can be wrapped to the desired shape and installed on the skeletal rod. Due to the lack of coarse aggregate and conventional reinforcement steel bars, it can be molded into any shape (Fayed et al., 2022; Naaman, 2000b). Due of the high specific surface area of ferrocement, the bonding forces between the mesh and cement mortar are quite strong (Varma & Hajare, 2015; Sakthivel & Jagannathan, 2012). Additionally, the closely spaced wire mesh serves as a crack-stopping feature and boosts the ductility of the ferrocement composite (Kumar, 2005; Navid et al., 2013). Numerous studies (Rajendran & Soundarapandian, 2015; Vickridge & Ranjbar 1998a; Vicridge & Ranjbar 1998b) used adjustment of mesh variation to enhance the properties of ferrocement mortar. In the experiments, galvanized wire mesh was used in place of steel wire mesh, and dense mortar was made using fly ash and silica fume admixture. The performance attributes of ferrocement composites are decreased as a result of these alterations, which served to increase the endurance of the ferrocement composites but become ineffective after a given amount of time. Utilizing polypropylene fabrics to reinforce ferrocement concrete has several benefits, including reduced corrosion, increased longevity, and reduced structural deterioration. The leftover components can also be used to create ferrocement composites (Dotto et al., 2004; Torri & Kawamura, 1990).

Polypropylene fibers' impact on ferrocement slab behavior was studied by Shri and Thenmozhi (Ramesht, 1995). The fiber content, the number of welded mesh layers, and the slab thickness served as the study's major criteria. The addition of polypropylene fibers boosted the slab's load capacity and the number of cracks, while reduced their breadth. Additionally, Hago et al. (Thenmozhi & Shri, 2012) studied the effect of the number of wire mesh layers on the initial crack load, ultimate flexural strength, and crack spacing of ferrocement roof slab panels. Many studies used ferrocement technology to strengthen, rehabilitate, and repair conventional RC beams, and it was an inventive way to increase the beam's strength (Al-Rifai et al., 2017; Baraghith, et al., 2022; Basha et al., 2020; Chandralekha & Surendar, 2016; Fayed

2019; Hago et al., 2005; Eswaran, 2016; Mansour & Fayed, 2021; Nahar et al., 2014; Shaheen et al., 2018).

It is well known that using lightweight aggregate concrete has a number of advantages, including a decrease in dead loads, cost savings on foundations and reinforcement, improved thermal properties, improved fire resistance, reduced need for formwork and props, and savings on transport and handling precast units on site. As a result, numerous researchers looked at hollow-core ferrocement members and lightweight concrete-filled lightweight concrete elements. Syahrul et al. (Yousry et al., 2018) investigated the behavior of composite beams made of lightweight foamed concrete (LFC) and traditional RC beams. The findings demonstrated that typical RC beams and LFC beams underwent nearly identical flexural processes, as well as LFC beams exhibiting ductile deflection behavior. Compared to normal-weight concrete, lightweight concrete can dramatically lower the dead load on structural concrete components (Syahrul et al., 2021). By substituting lightweight aggregates, such as lightweight aerated autoclaved crushed brick aggregate (LAABA), extruded foam, and expanded polystyrene (EP) aggregates for the heavy weight conventional coarse aggregates in the concrete mix, lightweight concrete has been created. The weight of concrete decreased by around 23% thanks to a well-designed lightweight concrete mix, while the ultimate strength rose by roughly 32.1% (Concrete made and with Different Types of Crushed Bricks, 2019). Many researchers approved that the use of steel or polypropylene fibers improved structural characteristics of normal-weight concrete and lightweight concrete beams and slabs (Ababneh et al., 2017; Alhassan et al., 2017, 2018; Al-Rousan, 2017, 2018a, 2018b, 2018c; Al-Rousan et al., 2018; Thiyab, 2016).

According to the findings of earlier studies in the literature, there are still a number of variables that have not been thoroughly investigated, such as totally replacing traditional stirrups with welded steel mesh, the type of infill material used for hollow core, and the hollow number. As a result, the structural performance of ferrocement beams with lightweight cores reinforced with steel mesh fabric as a shear reinforcement is the subject of this work. Expanded polystyrene and lightweight autoclaved brick aggregate were both used to create lightweight core concrete. The structural performance of the beams was tested for the effects of core lightweight concrete type, shape/number of holes, existing steel mesh fabric, concrete type, existing hollow core, and hole positioning. This study looked at structural performance variables, such as failure, cracking loads and deflections, and ultimate loads and deflections of the tested composite beams.

"Importance of Research" Section provides an illustration of the significance of the research, and "Experimental Program" Section includes an explanation of the experimental program's materials, specimens, and setup. Failure mechanisms, load–deflection response, cracking stage behavior, final stage behavior, ductility, stiffness, energy absorption of tested beams, and comparison with prior studies are all covered in "Results and Discussion" Section. Predictive models employing statistical analysis are explained in "Predictive Models Using Statistical Analysis" Section . "Conclusion" concludes with a summary and closed conclusion.

2 Importance of Research

As a cementitious component, ferrocement concrete is seen as a building material with the ability to satisfy the rising need for difficult, cost-effective, high-performing structures. Ferrocement concrete provides outstanding mechanical qualities, cracking control, and ductility, according to all prior investigations. Steel meshes of any size can be used to reinforce ferrocement concrete, which has the benefit of lowering the amount of tensile reinforcement needed in flexural components like beams, which increases the tensile strength of the structural elements. Additionally, the addition of steel meshes to the beams improved bending behavior since the beams' cracking pattern was composed of several fine, evenly spaced cracks, leading to a more ductile failure. Few studies have examined the potential use of lightweight aerated concrete enclosed in ferrocement for structural components. Additionally, no study substantiated the idea that lightweight cored ferrocement beams would be a viable alternative to conventional beams, particularly in low-cost housing constructions. In order to reduce weight without impairing the beam's resistance to flexure or shear, this research aims to liberate the interior longitudinal core from ferrocement beams and replace it with lightweight concrete. Additionally, sound and heat insulation were advantages of the lightweight concrete. Furthermore, this study examines the impact of various core materials on the structural performance of lightweight ferrocement composite beams.

3 Experimental Program
3.1 Materials
3.1.1 Concrete
3.1.1.1 Normal-weight Concrete In this experiment, conventional normal-weight concrete (NWC) mix with compressive strength of 25 MPa was employed to cast conventional structural beams. To create NWC mix, ordinary Portland cement, sand, crushed dolomite, and water are combined. The cement used complies with Portland cement type I and has a grade of 42.5. Additionally, the cement has a specific surface area per gram of 3050 cm^2. Local river sand, with natural siliceous, was used as the fine aggregate. It had a fineness modulus of 2.7, a specific gravity of 2.6 t/m^3, and was almost impure free. The coarse aggregate used was crushed dolomite with a specific gravity of 2.35 t/m^3. Sand and crushed dolomite have maximum nominal aggregate sizes of 2.5 mm and 19 mm, respectively. The water used to mix the concrete was safe to drink, devoid of contaminants that could have compromised the strength, and durability of the concrete. Table 1 lists proportions of normal-weight concrete (NWC) mix. During casting of NWC beams, three cubes (100 mm side) and cylinders (100×200 mm) were taken from the NWC mix to determine compressive and splitting tensile strengths. After 28 days, compressive and splitting tensile strengths of NWC were 25.5 and 2.5 MPa, respectively.

3.1.1.2 Ferrocement Concrete The proportions of the ferrocement concrete (FC) mix are reported in Table 1. Silica fume, fly ash, polypropylene (PP) fiber, ordinary Portland cement, water, sand, and superplasticizers are the main ingredients of FC mix. The amount of each ingredient in FC mix is calculated in accordance with ACI 549.1R-93 (Shaaban, 2002) to achieve the target compressive strength of 40 MPa.

To create a high-strength mortar, condensed silica fume in powder form with a light gray tint were employed in place of some of the cement. It was used to replace 10% of the cement's weight with silica fume. Additionally, a percentage of the fly ash is added to the cement. The employed fly ash conforms to pertinent international quality standards for fly ash as well as the chemical and physical requirements of ASTM C618.

Table 1 Proportions of mixes (kg/m^3)

Mix	Portland cement	fly ash	Silica fume	Fine aggregate	Coarse aggregate	Water	SP	PP Fiber	LAABA	EP aggregate
NWC	350	–	–	665	1330	130	–	–	–	–
FC	450	120	45	1200	–	275	12.2	1.2	–	–
BLWC	405	–	45	701	–	171	9	1.2	420	–
FLWC	450	–	45	500	–	205	6.75	–	–	23.5

SP is superplasticizers, *PP* is polypropylene fiber

Shaheen *et al. Int J Concr Struct Mater* (2023) 17:21

Page 5 of 24

ASTM C-1116 compliant polypropylene fibrillated (PP). Fibers made precisely to the best gradation for use as secondary reinforcement in concrete that contains no reprocessed hydrocarbon components. Application must be at least 0.9 kg per cubic meter. Fibers are typically utilized to prevent cracking brought on by drying shrinkage as well as thermal expansion and contraction. Additionally, it was employed to add fibers increase the toughness and residual strength, decrease concrete permeability, boost impact strength, raise shatter resistance, and increase abrasion resistance. In this work, the PP fiber was gradually added within the FC mix to prevent the threads from adhering to one another (agglomeration). PP fiber used is shown in Fig. 1. A high-range water reducer that satisfies ASTM C494 standards is utilized as a superplasticizer (trade name: Addicrete BVF; Modern Construction Chemicals Egypt) (types A and F). In hot regions, superplasticizers are utilized to generate high-quality concrete and give the concrete mix the essential workability. A brown liquid with a density of 1.18 kg/liter at room temperature is the admixture that is utilized. Three cubes (100 mm on each side) and cylinders (100×200 mm) were taken from the FC mix during the casting of FC beams to measure the compressive and splitting tensile strengths. FC had compressive and splitting tensile strengths of 36 and 3.5 MPa after 28 days, respectively.

3.1.1.3 Lightweight Concrete In this work, two lightweight concrete mixes are used to fill hollow core in the FC beams. First is made from lightweight aerated autoclaved brick aggregate (LAABA) as a course aggregate and this lightweight concrete is labeled by brick lightweight concrete (BLWC). However, the second is made from expanded polystyrene (EP) as a course aggregate and this lightweight concrete is labeled by expanded polystyrene (extruded foam) lightweight concrete (FLWC). LAABA is made from lightweight bricks with dimensions of $600 \times 200 \times 120$ mm, as shown in Fig. 2a, which commercially produced and used in constructing walls in residual building. The lightweight bricks had 650 kg/m3 as a unit weight. Moreover, the standard compressive test was carried out on three cubes ($150 \times 150 x150$ mm) that were cut from the lightweight bricks used and it was found that the average compressive strength was 2.5 MPa. To get LAABAs, depicted in Fig. 2b, full size bricks were manually crushed. The maximum nominal size of LAABAs is 10 mm. Table 1 lists all proportions of BLWC mix. This mix is consisting of Portland cement, silica fume, fine aggregate (sand), water, LAABA, superplasticizer, and PP fiber. Three standard cubes and cylinders (100×200 mm) were taken from this mix during the casting of hollow core to measure the compressive and splitting tensile strengths. BLWC mix had compressive and splitting tensile strengths of 11 and 1.2 MPa after 28 days, respectively.

Fig. 3 depicts expanded polystyrene (EP) or extruded foam (trade name: Addipor 55; Modern Construction Chemicals Egypt) which was used in manufacturing foam lightweight concrete (FLWC). The EP that was used contained ball-shaped granules with an approximate diameter of 1–2 mm. It has low thermal conductivity, good water permeability resistance, and a density of 30 kg/m^3, reported by the manufacturer.

Table 1 lists all proportions of FLWC mix. This mix is consisting of Portland cement, silica fume, sand, water, EP aggregate, and superplasticizer. Three standard cubes and cylinders were taken from this mix during the casting of hollow core to measure the compressive and splitting
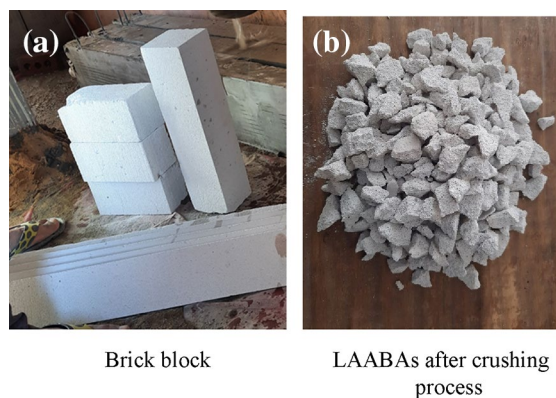

Fig. 1 PP fiber used in this work

Brick block   LAABAs after crushing process

Fig. 2 Lightweight aerated autoclaved brick aggregates (LAABAs)

Fig. 3 Expanded polystyrene (EP) aggregates

tensile strengths. FLWC mix had compressive and splitting tensile strengths of 5 and 0.45 MPa after 28 days, respectively.

Failure modes of cubes that made from FLWC, BLWC, FC, NWC, and brick block are shown in Fig. 4a–e. The best mode occurred in FC (Fig. 4c) due to existing PP fiber prevented the concrete to separate and high density of the mix improved the failure. However, the worst mode took place in NWC where almost cube completely crushed at maximum compression stress (Fig. 4d). The reason is that the failure occurred in dolomite particles which were weaker than the cement mortar. On the other hand, FC mortar did not include coarse aggregate. Because FLWC, BLWC, and brick blocks have air voids, they are very compressible under compression stress. As a result, the hair cracks on the vertical sides of the cubes occurred as well as preventing full crushing like NWC.

Failure modes of mixtures cylinders resulted from splitting tensile tests are shown in Fig. 5a–d. It was shown that both BLWC and NWC split once the load reach the peak, while both FC and FLWC did not split although the loading continued after the peak. This may be occurred because when the mix containing coarse aggregate, such as crushed dolomite or LAABA, the failure took place in the aggregate particles resulting in splitting mode. On contrast, addition PP fiber in FC mortar prevented splitting.
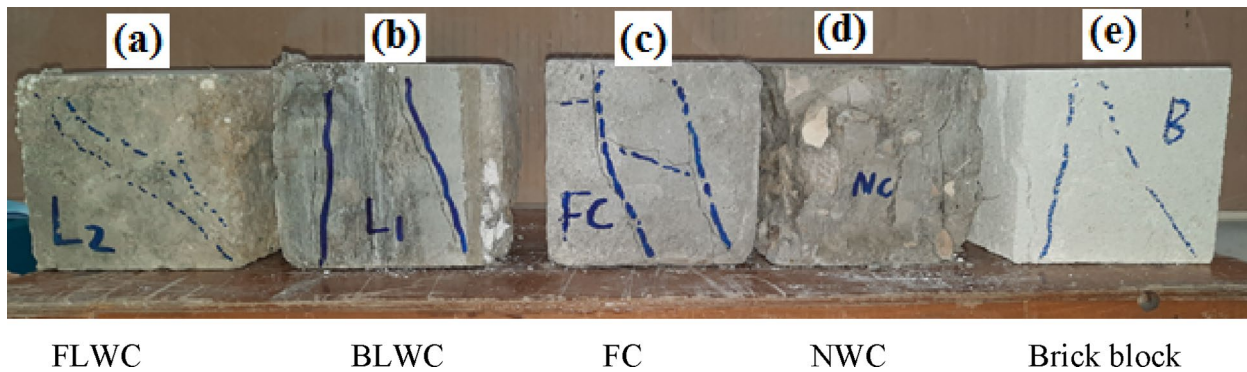

| FLWC | BLWC | FC | NWC | Brick block |

Fig. 4 Compression failure modes of all tested mixtures and brick block

| FLWC | BLWC | FC | NWC |
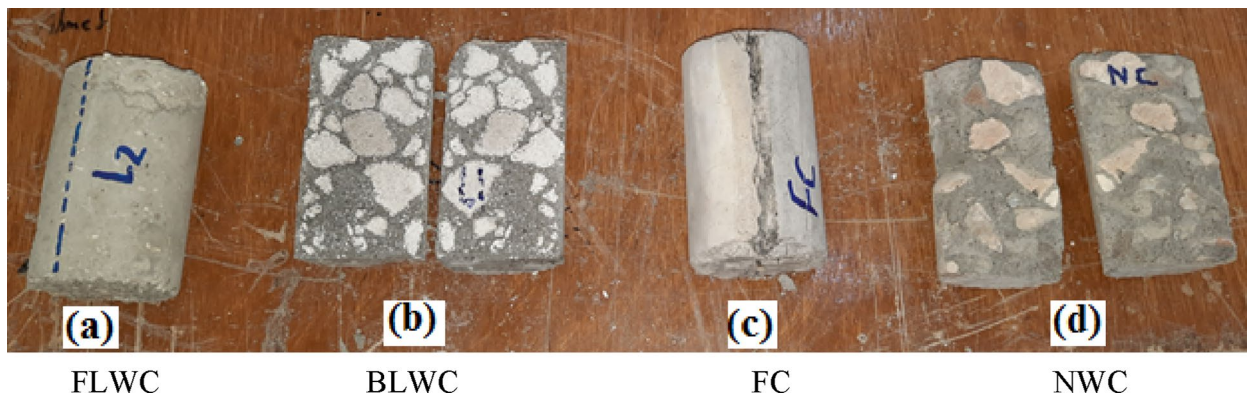
Fig. 5 Splitting tensile failure modes of all tested mixtures

Shaheen *et al. Int J Concr Struct Mater* (2023) 17:21

Page 7 of 24

Table 2 Elasticity modulus of all concrete mixtures

Concrete mix	W_c (kg/m³)	f_{cu} (MPa)	$f_c^/$(MPa)	E_c (MPa)
FLWC	1060	5	4	2967.95
BLWC	1770	11	8.8	9498.82
NWC	2500	25.5	20.4	24276.92
FC	2300	36	28.8	25454.02

During performing compression tests on all mixtures, weight of all cubes is obtained to understand difference in the mixture's weights. It was obtained that the weight of FLWC, BLWC, NWC, and FC is 1060, 1770, 2500, and 2300 kg/m³. Weight of FC was 8% less than that of NWC due to the absence coarse aggregate. Compared to NWC, weight of FLWC and BLWC decreased by 57.6 and 29.2%, respectively. Also, compared to FC, weight of FLWC and BLWC decreased by 53.9 and 23%, respectively. The elasticity modulus of each concrete mixture that has been presented needs to be determined. Elasticity modulus is important for designers and necessary in beams' serviceability limit states. Modules of elasticity of all concrete mixtures (E_c) are determined below according to AISC 360–10 (AISC 2010) (Shaaban., 2002):

$$\text{Ec} = 0.043 W_c^{1.5} \sqrt{f_c^/}, \tag{1}$$

where $f_c^/$ is the cylindrical compressive strength of the concrete ($f_c^/ = f_{cu}/1.25$), f_{cu} is the cubic compressive strength of the concrete which experimentally found in this work, and W_c is the weight of concrete per unit volume which was determined in the presented work. Table 2 lists values of Ec for all mixes.

3.1.2 Reinforcing Steel Bars
Both NWC and FC beams employed longitudinal reinforcing steel ribbed bars. The longitudinal bars utilized have a nominal yield and ultimate strength of 360 MPa and 500 MPa, respectively. The bars used have diameters of 10 and 12 mm. As a shear reinforcement in NWC beams, normal mild steel with a smooth surface and a diameter of 6 mm was used. These bars have an ultimate strength of 350 MPa and a nominal yield of 240 MPa, respectively.

3.1.3 Steel Mesh Reinforcement
Welded wire meshes (WWM) made from welded galvanized wires with diameter of 0.75 mm and with square openings of 12×12 mm size were used as a shear reinforcement in FC beams. Fig. 6 shows WWM photo. Weight of WWM is 450 kg/m². According to manufacturer, the mechanical properties of WWM in terms modulus of elasticity, proof stress, proof strain, ultimate
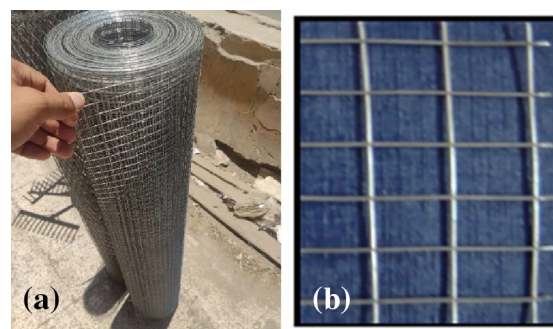

Full roll   Zoom shot on opening

Fig. 6 Welded wire mesh (WWM)

strength, and ultimate strain are 170 GPa, 400 MPa, 0.0012, 600 MPa, and 0.0058, respectively.

3.2 Beams Specimens
Experimental program consisted of 12 beams. Two of them made from NWC and ten made from ferrocement concrete (FC). Size, bottom tensile reinforcement, and top compression reinforcement are constant in all twelve beams. The beams have a width of 100 mm, a depth of 200 mm, and a total span of 2000 mm, while loaded length was 1900 mm. Two high tensile steel bars of 12 mm diameter were used as tension steel and two high tensile steel bars of 10 mm diameter were used as compression steel. Table 3 lists details of all beams. Details of two NWC beams A1 and A1 are drawn in Figs. 7 and 8, respectively. Two beams are similar in shear reinforcement which normal mild steel bar of 6 mm at pitch of 170 mm was used as stirrups along whole beam span. The difference between two beams is existing hole where beam A1 is solid with no hole (see Fig. 7) and beam A2 incorporated a circular hole of 50 mm diameter at the tension side (see Fig. 8).

Instead of using stirrups as a standard shear reinforcement, all 10 FC beams were strengthened with two layers of WWM. The longitudinal reinforcing cage of the beam is entirely encircled by these layers. Two NWC beam stirrups are equalized by choosing a two-layer amount. NWC/FC beam longitudinal reinforcement is comparable. Each of the ten FC beams has one or two holes. Additionally, two layers of WWM were used to reinforce and contain all holes in all beams. All FC beams had a circular opening with a diameter of 50 mm and with the exception of specimen C4, which had a rectangular opening with a cross-section of 40×50 mm. FC beams are depicted in longitudinal and cross-sectional views in Figs. 9 and 10, respectively. A circular hole is included into three beams B1, B2, and B3 on the tension side (Fig. 10a-c). B1's hole was empty and had no filler. While

Shaheen *et al. Int J Concr Struct Mater* (2023) 17:21

Page 8 of 24

Table 3 Details of the test specimens

| Beam	Concrete type	Shear Reinforce	Reinforcement steel bars		Hole condition	Hole size (mm)	Hole position	Filling material
			Tension steel bars	Compression steel bars				
A1			2Ø12	2Ø10	Solid	NA	NA	NA
A2	NWC	Stirrups Ø6@170 mm	2Ø12	2Ø10	One circular	Dia.50	Tension	No
B1	FC	Two layers of WWM	2Ø12	2Ø10	One circular	Dia.50	Tension	No
B2			2Ø12	2Ø10	One circular	Dia.50		BLWC
B3			2Ø12	2Ø10	One circular	Dia.50		FLWC
C1			2Ø12	2Ø10	One circular	Dia.50	Center	No
C2			2Ø12	2Ø10	One circular	Dia.50		BLWC
C3			2Ø12	2Ø10	One circular	Dia.50		FLWC
C4			2Ø12	2Ø10	Rectangular	40 × 50		BLWC
D1			2Ø12	2Ø10	Two circulars	Dia.50	One at Compression and one at tension	No
D2			2Ø12	2Ø10	Two circulars	Dia.50		BLWC
D3			2Ø12	2Ø10	Two circulars	Dia.50		FLWC
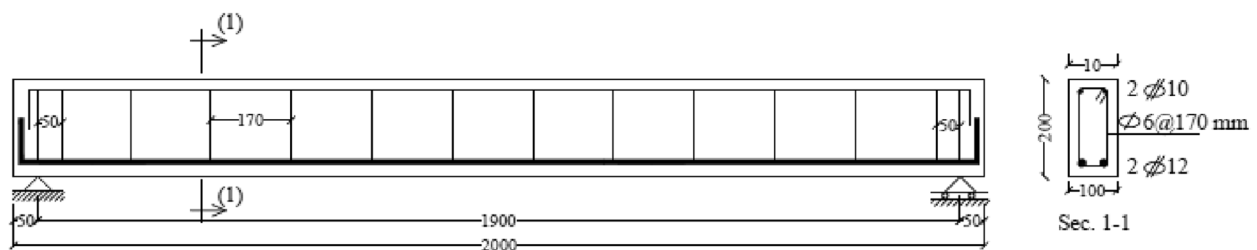
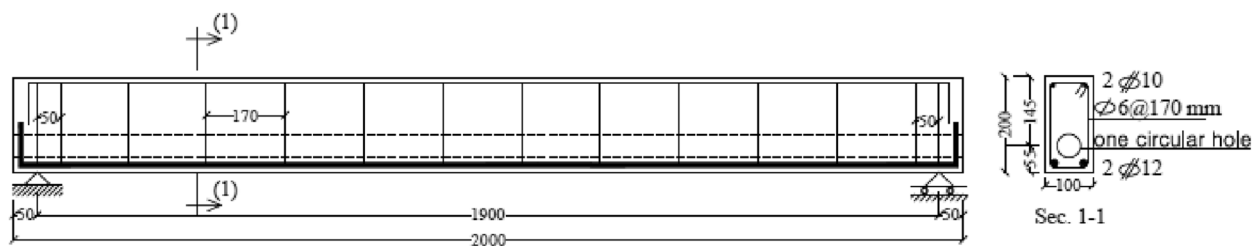**Fig. 7** Details of NWC beam (A1), dim in mm

Fig. 8 Details of NWC beam (A2), dim in mm

the hole of B3 is filling with FLWC, B2's hole is filling with BLWC. Four beams (C1, C2, C3, and C4) had a hole at the beam section's centroid (Figs. 10d–i). In contrast to beam C4, which featured a rectangular opening with a cross-section of 40 × 50 mm, beams C1, C2, and C3 all had circular holes. C1's hole was empty. With BLWC and FLWC, respectively, the holes of C2 and C3 are filled. BLWC is filling the C4 hole. Two 50-mm-diameter circular openings, one at the compression zone and the other at the tension side, were present in the three beams D,

D2, and D3 (Figs. 10m–s). Three beams' tension holes are empty, but D2 and D3's compression holes are filled with BLWC and FLWC, respectively. D1's compression hole is not filled.

FC beams' casting process is shown in Fig. 11. Three stirrups were utilized, as depicted in Fig. 11a, to alter the distribution of the bottom and top longitudinal bars and the toxicity. Reinforcing bars were covered in two layers of WWM (Fig. 11b). A PVC pipe with the same hole diameter was positioned in the desired location inside
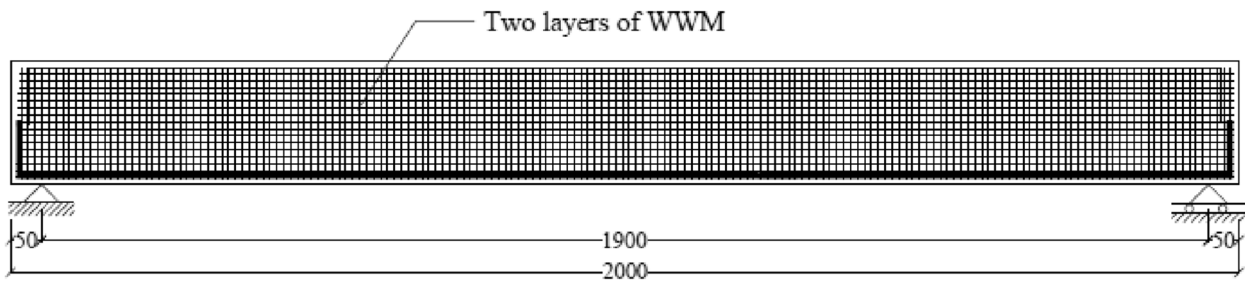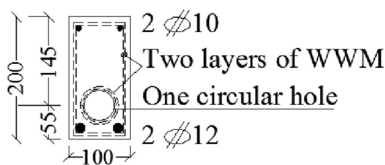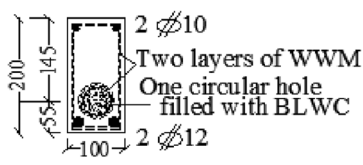
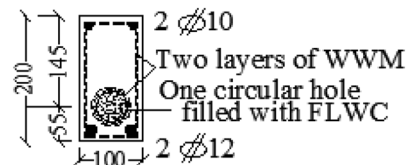**Fig. 9** Longitudinal cross section of FC beams, dim in mm

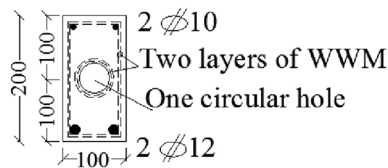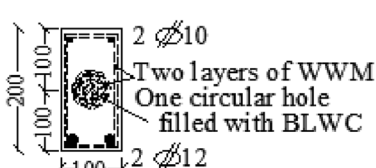

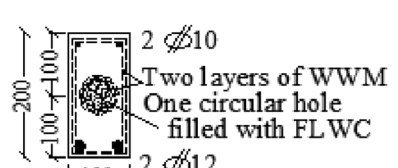**(a)** B1   **(b)** B2   **(c)** B3

(d) C1   **(e)** C2   **(h)** C3
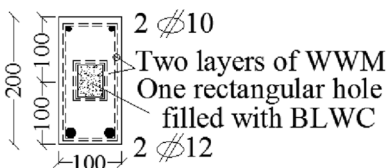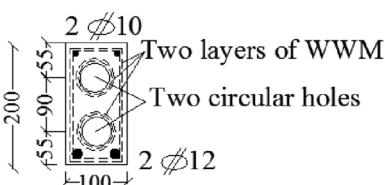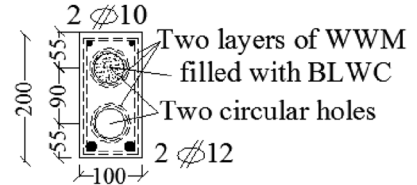
(i) C4   **(m)** D1   **(n)** D2
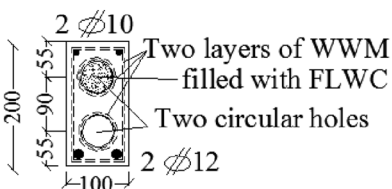
(s) D3

Fig. 10 Cross sections of FC beams, dim in mm
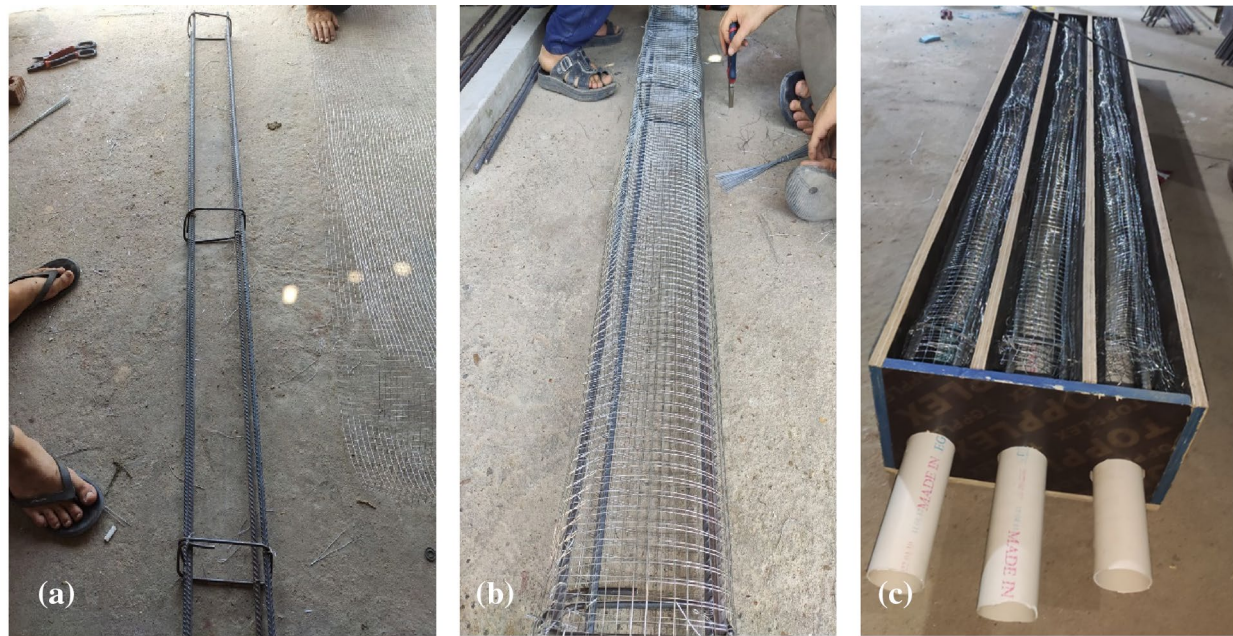
(a) Reinforcement bars   (b) Fabrications of WWM layers   (c) Wooden forms

(d) All beams after casting

Fig. 11 Casting process of FC beams

the beam in order to produce a longitudinal hole with a certain position in the section. To strengthen the hole, two layers of WWM were wrapped around the pipe. Inside wooden forms, the reinforcing cages and pipe were securely fastened. For instance, Fig. 11c illustrates the shapes of three beams, B1, B2, and B3. The concrete was then cast after that. This PVC pipe was removed after the concrete had hardened for 50 min. In Fig. 11a, d picture of every beam after casting is shown.

The specimens were weighed, while the experiments were being conducted. The test beams' weights are noted in Table 4. As can be observed, a 26% weight reduction was achieved when comparing conventional normal-weight concrete beams to those manufactured of lightweight ferrocement beams. The weight of the ferrocement beams filled with BLWC (B2, C2, C4, and D2) decreased by 10, 10, 10, and 19.11% in comparison to the solid NWC beam A1, whereas the weight of the

Table 4 Relative weight of specimens

Beam	A1	A2	B1	B2	B3	C1	C2	C3	C4	D1	D2	D3
Weight (kg)	100.00	90.19	82.97	89.92	87.13	82.97	89.92	87.13	89.88	73.95	80.89	78.11
% Weight reduction relative to A1	0.00	9.81	17.03	10.08	12.87	17.03	10.08	12.87	10.12	26.06	19.11	21.89

Fig. 12 Test setup and measurements, dim in mm

ferrocement beams filled with FLWC (B3, C3, and D3) decreased by 12.8, 12.8, and 21.89%, respectively.

3.3 Test Setup and Measurements
Fig. 12 depicts the test setup and instruments. A 1000 kN hydraulic jack that supplies the load at the middle of the tested beam is the major component. To prevent local concrete crushing failure, a 200×100 mm loading steel plate was positioned beneath the jack load. The ends of the beams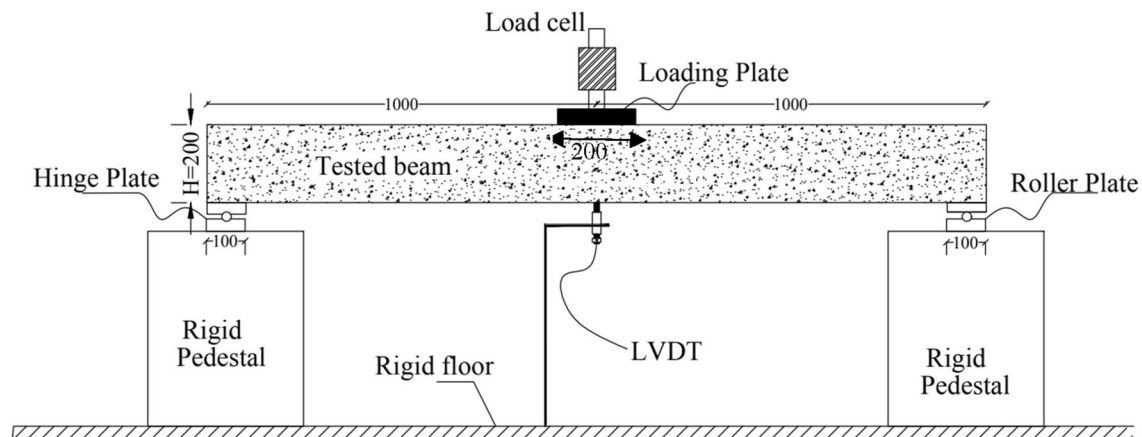 have hinged and roller supports. To record the load, a load cell was connected to the jack. The vertical mid-span deflection of the beam was measured with an LVDT (displacement transducer). Loading rate was 3 kN/min.

4 Results and Discussion
4.1 Failures Modes
The failure modes of each tested beam were displayed in Fig. 13. Table 5 contains the crack count and failure mode of the tested beams. Due to a large shear crack along the shear span, it was discovered that NWC beams (A1 and A2) failed in shear. Due to the lack of WWM and PP fiber, specimen A1 experienced the greatest shear brittle failure of all of the beams. Additionally, concrete crushing at the opening's sidewalls caused beam A2 to break. The number of cracks in FC beams was larger than in NWC beams (A1 and A2), proving the use of ferrocement concrete and the addition of WWM instead of

stirrups changed the failure mode from brittle shear to ductile tension flexure one. In a tension flexure failure, three beams (B1, B1, and B3) with a hole on the tension side failed. As opposed to B1 with an unfilled hole, B2 and B3 with lightweight concrete in the hole achieved a reduced cracks number. While C3 failed in shear flexure failure, C1 and C2 failed in flexure. This happened because the filler material in C2 (BLWC) is more efficient than the substance in C3 (FLWC). C4 was broke due to shear because a rectangular hole with dimensions of 40 mm in width and 50 mm in height resulted in a thin weak walls on two of its sides, which caused the section to break more quickly under light loads. Three beams D1, D2, and D3 exhibited a ductile flexure failure behavior.

4.2 Load–Deflection Response
To well understand effect of key variables on structural behavior of tested beams, all specimens were divided into groups: Group I which consisted of A1, A2, and B1 and investigate effect of existing opening, concrete type, and replacement of traditional stirrups by WWM; Group II which consisted of B1, B2, and B3 and studied effect of filling material type at tension side; Group III which consisted of C1, C2, and C3 and studied effect of filling material type at centroid of the section; Group IV which consisted of C2 and C4 and studied effect of hole shape (circular in C2 and rectangular in C4); Group V which consisted of B1 and D1 and studied effect of hole
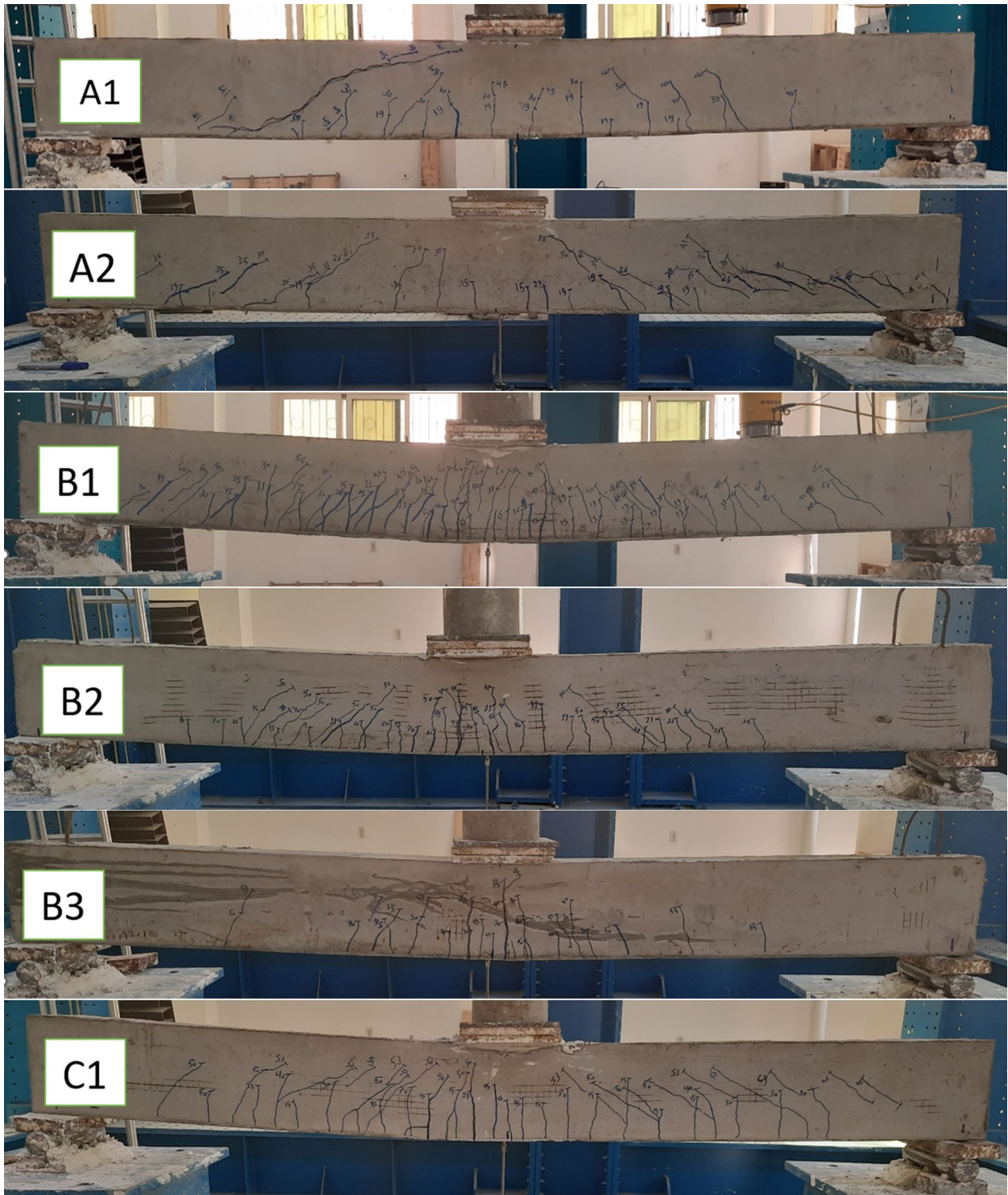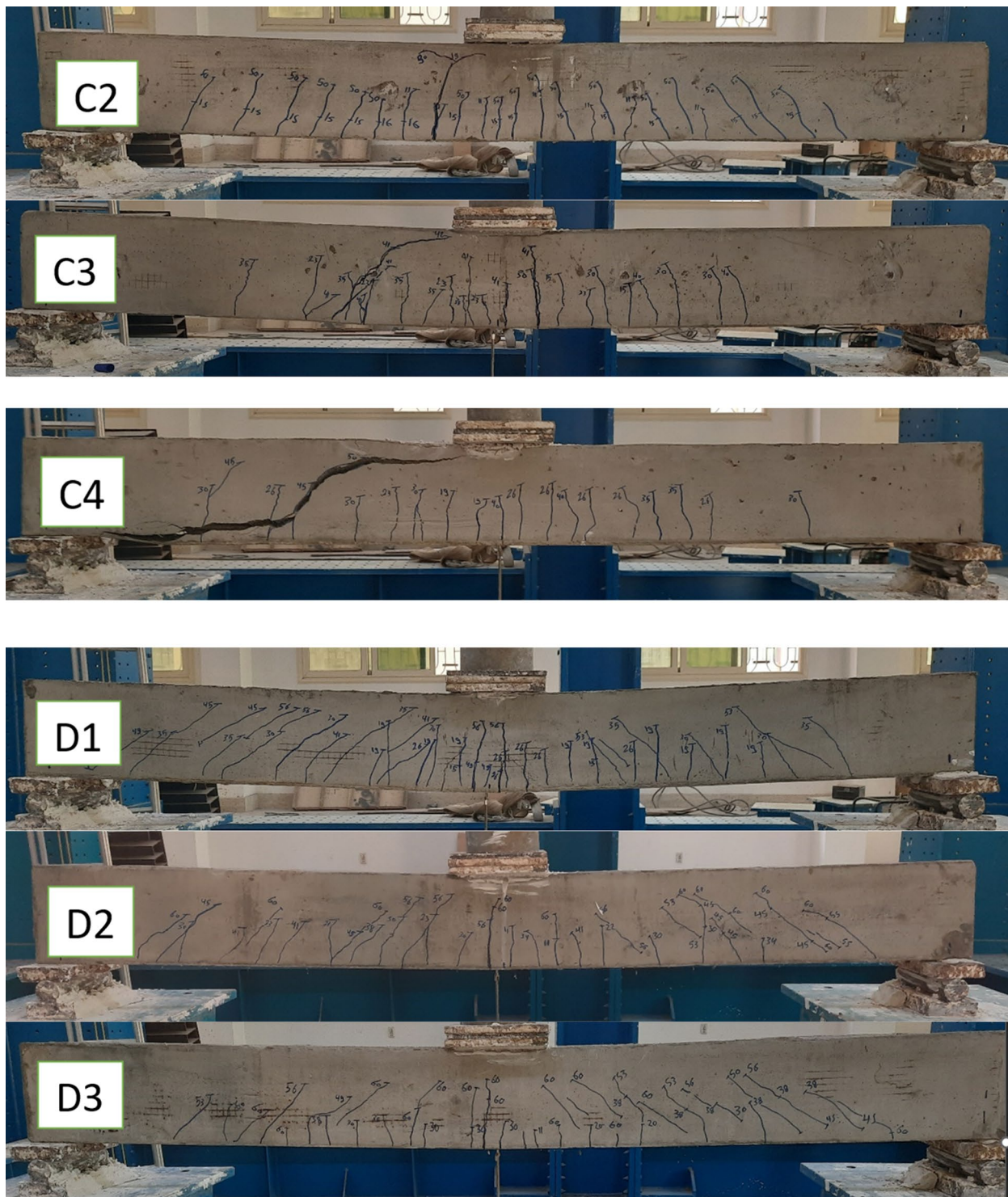
Fig. 13 The failure modes of all tested beams

Fig. 13 continued

number; and Group VI which consisted of D1, D2, and D3 and studied effect of filling material type at compression side.

Fig. 14 shows load–mid-span deflection curves of the beams. In general, the relationship of load and deflection is divided into four stages. Initial Phase I started from

Table 5 Test analysis

Beam	A1	A2	B1	B2	B3	C1	C2	C3	C4	D1	D2	D3
Failure	S	S	F	F	F	F	F	S-F	S	F	F	F
Cracks no	20	21	55	40	25	40	25	26	22	35	31	31

S is shear failure, *F* is tension flexure failure, *S-F* is shear flexure failure

beginning to first flexural crack and it is linear relationship. Phase II which is linear mode and started from first flexural crack to around 70–80% of ultimate load. With increase of loading (Phase III), the specimen exhibited a non-linear relationship with slight increase in load and high raise in deflection. This phase ended at the peak point. In Phase IV, curve of the specimen, that failed in shear, exhibited a brittle mode which suddenly dropped, while curve for the beam specimen, that failed in flexure, exhibited a ductile mode which horizontally continued after the peak for long deflection reached to 45 mm in some beams.

For Group I (Fig. 14a), existing 50 mm hole in tension side caused decline in carrying load at different deflection values as well as stiffness of beam A2 was less than A1. Behavior of FC beam B1 was much better than that of NWC beam A1 although the presence of hole in A1 due to ferrocement concrete quality and using WWM. For the rest Groups II–VI, using ferrocement concrete quality and using WWM as a shear reinforcement convert the brittle shear failure to ductile flexure failure. For Group II (Fig. 14b), no obvious improvement in the beam behavior occurred due to using filling materials in the hollow core placed at the tension side (BLWC in B2 and FLWC in B3) compared to control beam B1 with no fill. When the hole performed at the section center (Fig. 14c), Group III-beams behaved same trend of Group II-beams. From Fig. 14d, it was seen that performing circular hole that constructed in C2 was better than rectangular hole that constructed in C4. The effect of hole number on the load–deflection is shown in Fig. 14e. At all levels of deflection, specimen B1 containing one hole had a higher resisted load compared to specimen D1 containing two holes. In all beams containing two holes (D1, D2, and D3), no difference took place in the initial stiffness compared to specimen B1 containing one hole. On contrast, the effect of filling material in the hole positioned at the compression was remarkable (Fig. 14f). When the hole located in compression zone, using BLWC with $f_{cu} = 11$ MPa and FLWC with $f_{cu} = 5$ MPa to fill the hole empty improved significantly the beam behavior.

4.3 Cracking Stage Behavior
Almost structural member in the building was loaded up to service loads (around 50–60% of ultimate design loads). As a result, it is important to understand the effect of the main variables considered in this investigation on the structural behavior of the beams in terms of cracking loads and deflections. Moreover, the structural behavior of the beams at early stage is useful in studying serviceability limits. First flexure crack (Pcf) and corresponding deflection (Δcf) as well as first shear crack (Pcs) and corresponding deflection (Δcs) are observed during the experiments of the beams and listed in Table 6.

In general, Pcf to ultimate load (Pu) ratio was 0.4 and 0.2–0.3 for NWC and FC beams, respectively. It was well knowing that ferrocement concrete (FC) fast cracked from normal-weight concrete (NWC) due to existing coarse aggregate in the NWC mix. For Group I, existing hole in A2 and B1 declined the Pcf by 10.5 and 26.3% when referenced to solid beam A1, while hole improved the Δcf by around 40–47%. It was observed that hole decreased the gross area of the section hence the Pcf but the deformation improved. For Group II, the effect of filling material type of the hole at tension side caused a slight enhancement in the Pcf (7%), while it significantly declined deformation (36–71%). In three FC beams (C1, C2, and C3), the effect of filling material type at centroid of the section did not affect Pcf and Δcf. For Group IV, the effect of hole shape (circular in C2 and rectangular in C4) achieved a big difference in Pcf and Δcf. An increase of 37.5 and 911.8% occurred in Pcf and Δcf of the specimen C4 compared to C2. Additionally, it was seen that the effect of hole number did not affect Pcf and Δcf, as shown in Group V. Same trend occurred in filling material type at compression side, as shown in Group VI.

In general, Pcs to Pu ratio was 0.9–1.0 and 0.5–0.7 for NWC and FC beams, respectively. In two NWC beams (A1 and A2), once the load reached the Pu, the shear failure took place. However, almost FC beams failed in flexure collapse. For Group I, the Pcs of three beams A1, A2, and B1 was around 40 kN demonstrating that existing hole in A2 had no effect when referenced to solid beam A1. Also, demonstrating that using WWM companied to FC resisted same shear load of the NWC reinforced with traditional stirrups. Δcs of A2 was 38.4% less than that of A1. For Group II, the effect of filling material type of the hole at tension side caused a slight enhancement (2.5–5%) in the Pcs and caused a slight decline in the Δcs. Moreover, it was noticed that first shear crack

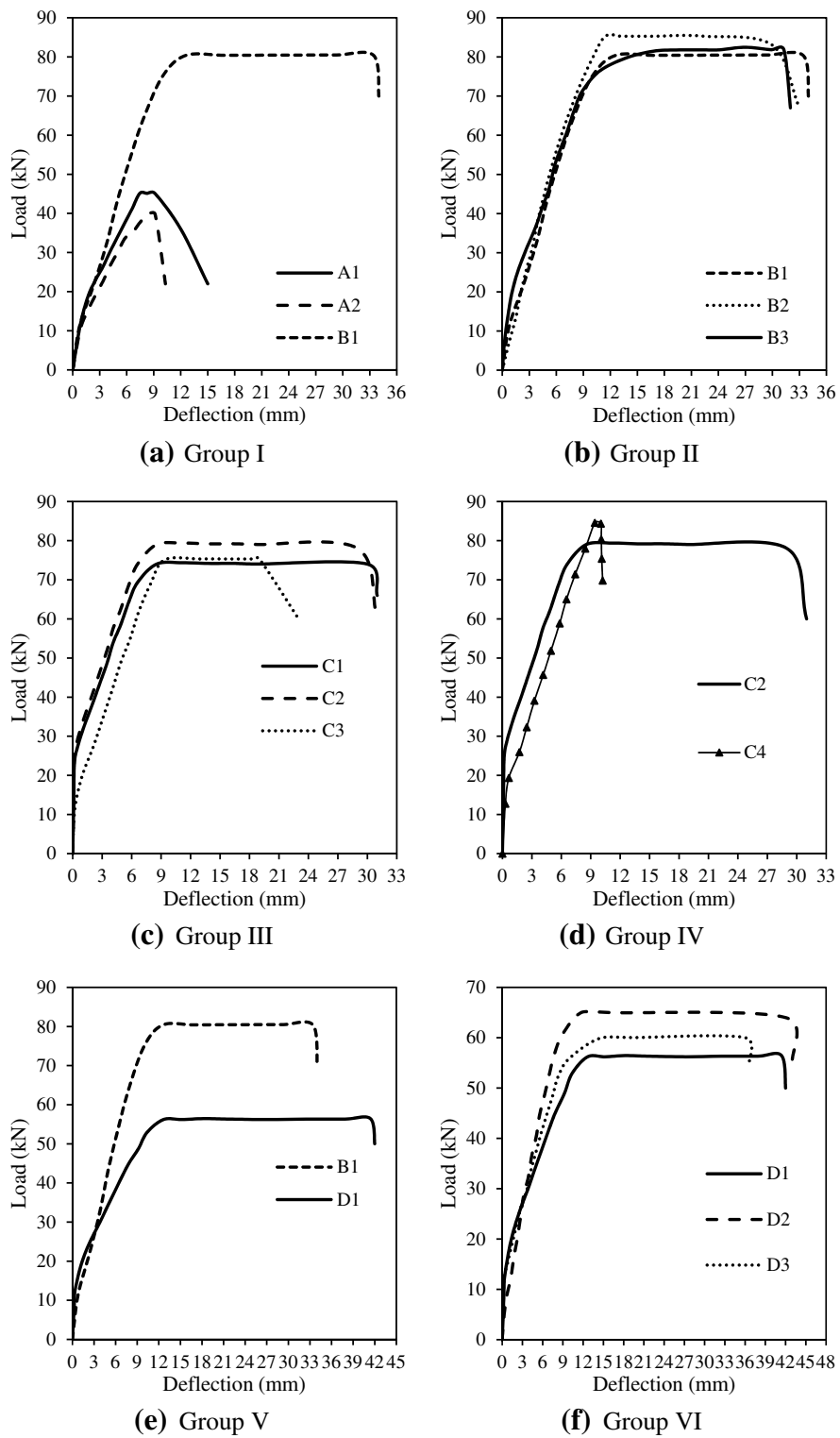Shaheen *et al. Int J Concr Struct Mater* (2023) 17:21

Page 15 of 24

Fig. 14 Load–mid-span deflection curves of the tested beams

Table 6 Results analysis at cracking stage

Beam	Pcf (kN)	Change in Pcf (%)	Δcf (mm)	Change in Δcf (%)	Pcs (kN)	Change in Pcs (%)	Δcs (mm)	Change in Δcs (%)
Group I: effect of existing opening, concrete type, replacement of traditional stirrups by WWM								
A1	19	0.0	1.7	0.0	41	0.0	6.61	0.0
A2	17	−10.5	2.5	47.1	41	0.0	9.15	38.4
B1	14	−26.3	2.38	40.0	40	−2.4	4.95	−25.1
Group II: effect of filling material type at tension side								
B1	14	0.0	2.38	0.0	40	0.0	4.95	0.0
B2	15	7.1	1.51	−36.6	42	5.0	4.53	−8.5
B3	15	7.1	0.69	−71.0	41	2.5	4.41	−10.9
Group III: effect of filling material type at centroid of the section								
C1	15	0.0	0.17	0.0	37	0.0	1.96	0.0
C2	16	6.7	0.17	0.0	39	5.4	1.96	0.0
C3	15	0.0	0.39	129.4	38	2.7	2.2	12.2
Group IV: effect of hole shape (circular in C2 and rectangular in C4)								
C2	16	0.0	0.17	0.0	39	0.0	1.96	0.0
C4	22	37.5	1.72	911.8	40	2.6	3.26	66.3
Group V: effect of hole number								
B1	14	0.0	2.38	0.0	40	0.0	4.95	0.0
D1	15	7.1	2.1	−11.8	40	0.0	3.89	−21.4
Group VI: effect of filling material type at compression side								
D1	15	0.0	2.1	0.0	39	0.0	3.89	0.0
D2	11	−26.7	2.05	−2.4	45	15.4	4.55	17.0
D3	11	−26.7	1.89	−10.0	41	5.1	4.8	23.4

(Pcs) did not approximately influence by filling material type at centroid/compression of the section, and shape/number of the hole. On the other hand, filling material type at centroid/compression of the section, and number of the hole caused a small change in the Δcs. On contrast, an increase of 66.3% occurred in Δcs of the specimen C4 containing a rectangular opening compared to C2 containing a circular opening.

4.4 Ultimate Stage Behavior
Ultimate load (Pu) and corresponding deflection (Δu) are listed in Table 7. In general, Pu of FC beams ranged from 56 to 85 kN, while Pu of control NWC beam A2 which includes hole was 41 kN. In other words, using FC mortar and different filling materials as well as replacement conventional stirrups by WWMs caused an increase (36.6–107.3%) in the Pu compared to control NWC beam A2. Additionally, the ultimate deflection (Δu) of FC beams was 9.42–33.1 mm, while it was only equal 8.9 mm in control NWC beam A2. In other words, Δu of FC beams increased by 6–272% compared to A2. These results proved that feasibility of the potential use of lightweight aerated concrete enclosed in ferrocement for structural components. Moreover, FC beams constructed with the presented production technology in

this research are better than NWC beams. In addition, weight of presented FC beams remarkability declined more than NWC beams.

For Group I, existing hole in A2 slightly declined the Pu by 9.1% when referenced to solid beam A1, while hole improved the Δu by around 17.1%. In addition, using lightweight aerated concrete enclosed in ferrocement in B1 significantly improved the Pu (increase = 78.3%) and the Δu (increase = 230.8%) when compared to A1. For Groups II and III, the effect of filling material type of the hole at tension side and centroid caused a slight enhancement in the Pu (1.5–6%), while it slightly declined ultimate deformation (10.2–23.1%) compared to similar reference specimens. For Group IV, the effect of hole shape achieved a slight difference in Pu while caused a big difference in the Δu. A decrease of 48.2% occurred in the Δu of the specimen C4 compared to C2. Additionally, it was seen that the presence of two holes in D1 declined the Pu by 30. % when referenced to B1 containing one hole, as shown in Group V. This was occurred because of weakness of the section resulting from holes declined the flexure rigidity; hence, the final capacity decreased. As shown in Group VI, a slight improvement took place in the Pu of D2 and D3 compared to D1. Generally, Pu of FC beams containing BLWC (B2, C2, C4, and D2) was

Table 7 Results analysis at ultimate stage

Beam	Pu (kN)	Change in Pu (%)	Δu (mm)	Change in Δu (%)	Δy (mm)	μ	Change in μ (%)
Group I: effect of existing opening, concrete type, replacement of traditional stirrups by WWM							
A1	45.12	0.0	7.6	0.0	3	2.53	0.0
A2	41	−9.1	8.9	17.1	3.05	2.9	15.3
B1	80.44	78.3	25.14	230.8	3.5	7.18	183.8
Group II: effect of filling material type at tension side							
B1	80.44	0.0	25.14	0.0	3.5	7.18	0.0
B2	85.3	6.0	21.4	−14.9	3.45	6.2	−13.6
B3	81.9	1.8	19.34	-23.1	3.2	6.04	−15.9
Group III: effect of filling material type at centroid of the section							
C1	74.18	0.0	16.51	0.0	0.5	33.0	0.0
C2	79.37	7.0	18.2	10.2	0.5	36.4	10.3
C3	75.32	1.5	12.9	−21.9	0.7	18.4	−44.2
Group IV: effect of hole shape (circular in C2 and rectangular in C4)							
C2	79.37	0.0	18.2	0.0	0.5	36.4	0.0
C4	84.5	13.0	9.42	−48.2	1.7	5.54	−84.8
Group V: effect of hole number							
B1	80.44	0.0	25.14	0.0	3.5	7.18	0.0
D1	56.2	−30.1	32.2	28.1	1.1	29.3	307.7
Group VI: effect of filling material type at compression side							
D1	56.2	0.0	32.2	0.0	1.1	29.3	0.0
D2	65	15.7	33.1	2.8	1.5	22.1	−24.7
D3	60	6.8	19.56	−39.3	1.3	15.0	−48.6

higher than that of FC beams containing FLWC (B3, C3 and D3). This was occurred because the compressive strength of BLWC mixture was 11 MPa, while the compressive strength of FLWC mixture was only 5 MPa. Also, it was found that when the filling material placed at the compression (D2 and D3), the improvement in the Pu was higher than when the filling material placed at the tension (B2 and B3) and at the centroid (C2 and C3). This was occurred because the concrete in tension side is neglected after the cracking; hence, it did not affect the final ultimate load (Pu).

4.5 Ductility Index

Even if the results of the preceding section showed that lightweight aerated concrete contained in ferrocement mortar could be used for ultimate loads, ductility response research is still crucial and necessary. Ductility index (μ) refers to ductile performance of the beam element. Eq. (2) was used to estimate μ:

$$\mu = \frac{\Delta_u}{\Delta_y}, \tag{2}$$

where Δu and Δy are ultimate deflection at the ultimate load (Pu) and the displacement at the yielding, respectively. Fig. 15 illustrates determining procedure of these

deflections Δu and Δy (Aksoylu et al. 2020). The μ of the tested beams are estimated and listed in Table 7.

In general, μ of FC beams ranged from 5.54 to 36.4, while μ of control NWC beam A2 was 2.9. In other words, using FC mortar and different filling materials as well as replacement conventional stirrups by WWMs caused a significant increase (89–1155%) in the μ compared to control NWC beam A2. Demonstrating possibility of using lightweight aerated concrete enclosed in ferrocement mortar for enhancing deformability as well as ultimate capacity. For Group I, existing hole in A2 slightly improved the μ by 15.3% when referenced to solid beam A1. Also, using lightweight aerated concrete enclosed in ferrocement in B1 significantly improved the μ (increase = 183.8%) when compared to A1. For Group II and III, the effect of filling material type of the hole at the tension side and centroid slightly declined the μ (13.6–44%) compared to similar reference specimens. For Group IV, the effect of hole shape caused a significant decline in the μ. A decrease of 84.8% occurred in the μ of the specimen C4 compared to C2. Additionally, it was seen that the presence of two holes in D1 increased the μ by 307.7% when referenced to B1 containing one hole, as shown in Group V. As shown in Group VI, a decrease took place in the μ of D2 and D3 compared to D1 when the hole was filled by different lightweight concretes.
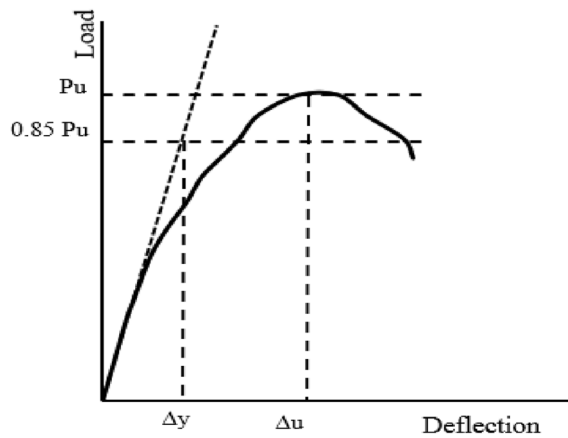
Fig. 15 Typical P–Δ curve; calculation method of ductility index of the tested beams (Aksoylu et al., 2020)

Generally, the ductility index of FC beams containing BLWC and FLWC (B1, B2, C3, C4, D2, and D3) was less than that of similar reference FC beams with no fill (B1, C1, and D1), showing that filling the holes negatively affect the ductility of FC beams (Fig. 15).

4.6 Stiffness and Energy Absorption

Table 8 lists values pre-/post-cracking stiffness (k) and energy absorption (EA) for all specimens. It was seen that pre-cracking energy absorption (EA_i) of A1 and B1 is similar, showing FC beams behaved same trend. EA_i of B2 and B3 was 32 and 68.9% less than that of B1 due to existing filler inside hollow. EA_i C4 with rectangular hollow was higher than C2 with circular hole. Number of holes slightly declined EA_i. EA_i of D2 and D3 with two filled holes was slightly decreased compared to D1. On the other hand, it was shown that post-cracking energy absorption (EA) depended on failure mode of the beams. When failure mode did not change, EA did not affect (Groups V and VI). When failure mode changed from shear to flexure, an increase of 380.2% (B1) took place in EA. On contrast, when failure mode changed from flexure to shear, a decline of 76% (C4) took place in EA. Also, when failure mode changed from flexure to flexure shear, a decline of 32% (C3) took place in EA.

It was seen that pre-cracking stiffness (k_i) of FC beam B1 was less than that of NWC beam A1 due to the absence of coarse aggregate in FC. In addition, when filler

Table 8 Results of Energy absorption and stiffness

Beam	Energy absorption (EA)					Stiffness (k)			
	EA_i (kN.mm)	Change in EA_i (%)	EA (kN.mm)	Change in EA (%)	Failure	k_i (kN/mm)	Change in k_i (%)	k (kN/mm)	Change in k (%)
Group I: effect of existing opening, concrete type, replacement of traditional stirrups by WWM									
A1	32.3	0.0	486	0.0	S	11.2	0.0	5.0	0.0
A2	42.5	31.6	278	−42.8	S	6.8	−39.2	4.5	−10.0
B1	33.3	3.2	2334	380.2	F	5.9	−47.4	4.4	−12.0
Group II: effect of filling material type at tension side									
B1	33.3	0.0	2334	0.0	F	5.9	0.0	4.4	0.0
B2	22.7	−32.0	2370	1.5	F	9.9	68.9	6.2	40.9
B3	10.4	−68.9	2262	−3.1	F	21.7	269.6	7.5	70.5
Group III: effect of filling material type at centroid of the section									
C1	2.6	0.0	2114	0.0	F	40.0	0.0	23.0	0.0
C2	2.7	6.7	2248	6.3	F	38.0	−5.0	21	−8.7
C3	5.9	129.4	1438	−32.0	S-F	32.0	−20.0	19.2	−16.5
Group IV: effect of hole shape (circular in C2 and rectangular in C4)									
C2	2.7	0.0	2248	0.0	F	38.0	0.0	21	0.0
C4	37.8	1291.2	538	−76.1	S	12.8	−66.3	9.3	−55.7
Group V: effect of hole number									
B1	33.3	0.0	2334	0.0	F	5.9	0.0	4.4	0.0
D1	31.5	−5.5	2122	−9.1	F	6.0	2.0	4.2	−4.5
Group VI: effect of filling material type at compression side									
D1	31.5	0.0	2122	0.0	F	6.0	0.0	4.2	0.0
D2	22.6	−28.4	2522	18.9	F	5.4	−10.6	4.4	4.8
D3	20.8	−34.0	1976	−6.9	F	5.8	−3.0	4.6	9.5

EA_i and EA are energy absorption before and after cracking, respectively, which are estimated by area under load–deflection curve for each beam. k_i and k are stiffness before and after cracking, respectively, which are estimated by slope of load–deflection curve for each beam. S and F are referring to shear and flexure failure

Table 9 Characteristics and ultimate loads of beams presented in the current work and previous studies

Source	Specimen ID	Specimen type	Number of layers	Type of mesh	Core configuration	P_u (kN)	Increase in P_u (%)
(Fahmy et al., 2014)	A1*	Beam	No	No	No	35.76	0.00
	B2		2	Expanded metal mesh	AAC	40.98	14.60
	B4		4	Welded wire mesh	AAC	46.19	29.17
	G2		2	Expanded metal mesh	EFC	37.19	4.00
	F1		1	Expanded metal mesh	LWC	40.95	14.51
	F2		2	Expanded metal mesh	LWC	38.75	8.36
	F4		4	Welded wire mesh	LWC	39.87	11.49
(Shaheen et al., 2020a)	O2*	Slab	No	No	No	34	0.00
	E1		1	Expanded metal mesh	No	38	11.76
	W2		2	Welded wire mesh	No	38	11.76
	W3		3	Welded wire mesh	No	42	23.53
(Abdullah & Abdull, 2022)	BNC*	Beam	No	No	No	42.2	0.00
	SBWS1		1	Welded wire mesh	No	46.6	10.43
	SBWS2		2	Welded wire mesh	No	50.5	19.67
	SBWS3		3	Welded wire mesh	No	55.9	32.46
Current study	A2*	Beam	No	No	No	41	0.00
	B1		2	Welded wire mesh	No	80.44	96.20
	B2		2	Welded wire mesh	BLWC	85.3	108.05
	B3		2	Welded wire mesh	FLWC	81.9	99.76
	C1		2	Welded wire mesh	No	74.18	80.93
	C2		2	Welded wire mesh	BLWC	79.37	93.59
	C3		2	Welded wire mesh	FLWC	75.32	83.71
	C4		2	Welded wire mesh	BLWC	84.5	106.10
	D1		2	Welded wire mesh	No	56.2	37.07
	D2		2	Welded wire mesh	BLWC	65	58.54
	D3		2	Welded wire mesh	FLWC	60	46.34

AAC is Autoclaved Aerated lightweight brick Core, *EFC* is Extruded Foam Core, and *LWC* is Lightweight Concrete Core

* is control normal-weight concrete specimen

material existed at tension side (B1, B2, and B3) k_i significantly increased while it existed at the centroid (C1, C2 and C3) or at the compression side (D1, D2 and D3), k_i did not affect. It was seen that hole's number slightly affect k_i. On the other hand, it was shown that post-cracking stiffness (k) was slightly influenced by studied parameters.

4.7 Comparison with Previous Studies

In this study, FC beams' ultimate load results were compared to FC beam and slab testing results from earlier studies (Aksoylu et al., 2020; Fahmy et al., 2014; Shaheen et al., 2020a). Table 9 shows characteristics and ultimate loads of beams presented in the current work and previous studies. For the construction of FC beams and slabs, it was discovered that the combination of steel meshes and ferrocement mortar is a suitable substitute for normal-weight concrete elements. Ultimate load increasing ratios ranged from 4 to 29% in Fahmy et al. (2014) and from 11 to 23% in Shaheen et al., 2020a. Increased ratios

of the ultimate load in Abdullah and Abdull (2022) varied from 10 to 32%. Notably, control beams A1, O2 and BNC (Aksoylu et al., 2020; Alnuaimi et al., 2008; Fahmy et al., 2014) were collapsed due to flexural failure and all FC beams also failed in flexure. As a result, main role of steel meshes for enhancing the shear capacity did not appear; hence, increasing ratios were small. However, due to the control beam A2 failing due to shear, increasing ratios of the ultimate load ranged from 37 to 108% in the current work. It was shown that effect holing and filler had insignificant impact on the ultimate load.

5 Predictive Models Using Statistical Analysis

The results of this research and other investigations (Aksoylu et al., 2020; Fahmy et al., 2014; Shaheen et al., 2020a) were subjected to linear multiple regressions in order to derive new formulas that could estimate the ultimate load (Pue) and ultimate bending moment capacity (Mue) for all beams investigated in this research and other investigations. Pue is experimental ultimate load according

to each study, while Mue is estimated according to specimen setup that specified in each study. Multiple regressions were investigated using Excel data analytics. This analytical model is focusing on ferrocement flexural members (beams and slabs) reinforced with high tensile steel bars in the tension, provided with steel meshes either welded wire mesh (WWM) or expanded metal mesh (EMM), as well as contained hollow core either empty or filled with lightweight concrete. The input variables taken into consideration for the current analysis are compressive strength of ferrocement specimen either beams or slabs (f_{cus}), compressive strength of filling lightweight concrete of the hole (f_{cuh}), hole area-to-cross-sectional area of the specimen ratio (ψ_h), tensile reinforcement ratio (μ_t), and volume fraction of the steel mesh (V_m). Equation (3) was used to find the μ_t:

$$\mu t = \frac{A_s}{bd}, \tag{3}$$

where A_s is the tensile reinforcement (mm^2), b is the specimen width (mm), and d is the effective depth of the section (mm).

Equation (4) was used to find the V_m:

$$Vm = \frac{v_m}{v_s}, \tag{4}$$

where v_m is total volume of steel mesh (mm^3) which is estimated from Eq. (4) and v_s is total volume of specimen either beam or slab (mm^3).

$$v_m = \frac{NW_m}{\gamma_s}, \tag{5}$$

where N is layer number of steel meshes, γ_s is steel density which is taken by 7850 kg/m^3, and W_m is total weight of the one layer of steel mesh which is estimated from Eq. (5):

$$W_m = A_m w_m, \tag{6}$$

wherewherew_m is weight of steel mesh per one square meter (kg/m^2) which is mentioned in each study and A_m is total area of steel mesh performed in one specimen which was calculated from the specimen geometry in each study. All input data required in this regression process are obtained and listed in Table 10.

The theoretical ultimate load (Put) and theoretical ultimate moment (Mut) were chosen as the output parameters. There were 120 different input data sets in all (5 columns and 24 rows, as shown in Table 10). To get the best possible fit between the input and output parameters, many models were tested. The best equations for forecasting the Put and Mut, respectively, are (7) and (8):

$$Put = 57.817 - 0.145(f_{cus}) + 40.95(\mu_t) - 1.255(\psi_h) - 0.176(f_{cuh}) - 26.24(V_m), \tag{7}$$

$$Mut = 28.07 + 0.114(f_{cus}) + 13.568(\mu_t) - 0.633(\psi_h) - 0.093(f_{cuh}) - 12.78(V_m). \tag{8}$$

R^2 values of 0.879 and 0.897 for Eqs. (7) and (8) correspondingly showed good agreement. A correlation between experimental and anticipated values of the Put and Mut is shown in Table 11.

Equations. (7) and (8) can be used with confidence to forecast the ultimate load and bending moment capacity of hollow-core ferrocement concrete beams/slabs reinforced with steel meshes as a shear reinforcement since they are accurate for a wide variety of input variables, including f_{cus}, f_{cuh}, ψ_h, μ_t, and V_m.

6 Conclusion

In order to examine the structural performance of lightweight ferrocement hollow-core beams subjected to three-point flexure loading up to failure, this research is an experimental investigation made up of twelve reinforced beams. The beams are 100, 200, and 2000 mm in width, depth, and length, respectively, with a 1900 mm loaded span. Two 12-mm-high tensile steel bars were utilized to reinforce the bottom of the beams at a ratio of 1.13%. The shear reinforcement and concrete type of the beams differed. Two reference beams were constructed using conventional normal-weight concrete (NWC) and stirrups for shear reinforcement. One of them was solid and the other was hollow. The shear reinforcement of ten FC beams was provided by two layers of welded wire mesh (WWM). Three of them had had a circular hole (diameter: 50 mm) at the tension side, three had a circular hole (diameter: 50 mm) at the centroid, and one had a rectangular hole (width: 40 mm and height: 50 mm) at the centroid. Two circular holes (each measuring 50 mm in diameter), one at the tension and the other at the compression, are present in three beams. The hollow core in the FC beams is filled with two lightweight concrete mixtures. The first is built of lightweight aerated autoclaved brick aggregate and is called brick lightweight concrete (BLWC). While the second is built of expanded polystyrene and is called foam lightweight concrete (FLWC). In each set of beams, one beam had an empty hole, while the other beams' holes were filled by BLWC or FLWC, respectively. The primary influencing factors are the kind of lightweight concrete used for the hollow core, the size and number of holes, the type of concrete, the presence of a hollow core, and the existing steel mesh fabric. The ductility of the tested beams as well as failure mechanisms, cracking loads and deflections, and

Table 10 Input data set required for predictive model

Source	Specimen ID	Specimen type	Pue (kN)	Mue (kN.m)	f_{cus} (MPa)	μ_t (%)	ψ_h (%)	f_{cuh} (MPa)	V_m (%)
(Fahmy et al., 2014)	B2	Beam	40.98	18.44	35.5	1.13	25	2.5	1.03
	B4		46.19	20.79	35.5	1.13	25	2.5	0.64
	G2		37.19	16.74	35.5	1.13	25	5	1.03
	F1		40.95	18.43	35.5	1.13	25	24	0.52
	F2		38.75	17.44	35.5	1.13	25	24	1.03
	F4		39.87	17.94	35.5	1.13	25	24	0.64
(Shaheen et al., 2020a)	E1	Slab	38	22.78	35	0.26	13.08	0	0.34
	W2		38	22.78	35	0.26	13.08	0	0.23
	W3		42	25.17	35	0.26	13.08	0	0.34
(Abdullah & Abdull, 2022)	SBWS1	Beam	46.6	27.93	47	0.45	0	0	0.22
	SBWS2		50.5	30.27	47	0.45	0	0	0.43
	SBWS3		55.9	33.51	47	0.45	0	0	0.65
	BWS1		44.9	26.91	47	0.45	18.52	2	0.22
	BWS2		49.5	29.67	47	0.45	18.52	2	0.43
Current study	B1	Beam	80.44	38.21	36	1.13	9.8125	0	0.36
	B2		85.3	40.52	36	1.13	9.8125	11	0.36
	B3		81.9	38.90	36	1.13	9.8125	5	0.36
	C1		74.18	35.24	36	1.13	9.8125	0	0.36
	C2		79.37	37.70	36	1.13	9.8125	11	0.36
	C3		75.32	35.78	36	1.13	9.8125	5	0.36
	C4		84.5	40.14	36	1.13	10	11	0.36
	D1		56.2	26.70	36	1.13	19.625	0	0.36
	D2		65	30.88	36	1.13	19.625	11	0.36
	D3		60	28.50	36	1.13	19.625	5	0.36

ultimate loads and deflections were investigated. The key finding based on the experimental findings is as follows:

1) The use of ferrocement concrete and the installation of WWM in place of stirrups changed the failure mode from brittle shear, which happened in NWC beams, to ductile tension flexure mode, as evidenced by the fact that the number of cracks in FC beams was significantly higher than in NWC beams. First flexure crack to ultimate load ratios for NWC and FC beams were 0.4 and 0.2–0.3, respectively, while first shear crack to ultimate load ratios for NWC and FC beams was 0.9–1.0 and 0.5–0.7.

2) In NWC and FC beams, including hole at tension side (10% of area section), the first flexure crack was reduced by 10.5 and 26.3%, respectively, in comparison to solid NWC beams.

3) When compared to a control NWC beam, the employment of FC mortar, various filler materials, and WWMs in place of conventional stirrups increased the ultimate load by 36.6–107.3%, the ultimate deflection by 6–272%, and the ductility by 89–1155%.

4) When compared to a solid NWC beam, using lightweight aerated concrete enclosed in ferrocement dramatically increased the ultimate load (increase = 78.3%) and the ultimate deflection (increase = 230.8%).

5) The ultimate load and ultimate deflection were marginally impacted by filling material type compared to comparable control FC beams.

6) Due to BLWC's greater compressive strength than FLWC, FC beams containing BLWC had a higher ultimate load than FC beams containing FLWC.

7) Filling materials (BLWC and FLWC) of the hole at tension side and centroid of FC beams declined the ductility by around 13.6–44% compared to similar reference specimens.

8) When compared to FC beams with one hole (10% of the section), the presence of two holes (20% of the section) enhanced the ductility by 307.7%.

9) Energy absorption and initial stiffness of FC beams were 380% higher and 47% less than that of NWC control beams.

10) Since they are accurate for a wide range of input variables, such as compressive strength of the beam

Table 11 Values of theoretical ultimate load and moment versus experimental ones

Source	Specimen ID	Ultimate load			Ultimate moment		
		Pue (kN)	Put (kN)	Put/Pue	Mue (kN.m)	Mut (kN.m)	Mut/Mue
(Fahmy et al., 2014)	B2	40.98	40.05	0.98	18.44	18.20	0.99
	B4	46.19	50.28	1.09	20.79	23.19	1.12
	G2	37.19	39.61	1.07	16.74	17.97	1.07
	F1	40.95	49.81	1.22	18.43	22.80	1.24
	F2	38.75	36.27	0.94	17.44	16.20	0.93
	F4	39.87	46.50	1.17	17.94	21.19	1.18
(Shaheen et al., 2020a)	E1	38.00	38.11	1.00	22.78	22.97	1.01
	W2	38.00	41.15	1.08	22.78	24.45	*1.07*
	W3	42.00	38.18	0.91	25.17	23.01	0.91
(Abdullah & Abdull, 2022)	SBWS1	46.60	63.64	1.37	27.93	36.73	1.32
	SBWS2	50.50	57.96	1.15	30.27	33.96	1.12
	SBWS3	55.90	52.28	0.94	33.51	31.20	0.93
	BWS1	44.90	40.05	0.89	26.91	24.82	*0.92*
	BWS2	49.50	34.37	0.69	29.67	22.05	0.74
Current study	B1	80.44	77.13	0.96	38.21	36.70	0.96
	B2	85.30	75.19	0.88	40.52	35.68	0.88
	B3	81.90	76.25	0.93	38.90	36.24	0.93
	C1	74.18	77.13	1.04	35.24	36.70	1.04
	C2	79.37	75.19	0.95	37.70	35.68	0.95
	C3	75.32	76.25	1.01	35.78	36.24	1.01
	C4	84.50	74.96	0.89	40.14	35.56	0.89
	D1	56.20	64.81	1.15	26.70	30.49	1.14
	D2	65.00	62.88	0.97	30.88	29.47	0.95
	D3	60.00	63.93	1.07	28.50	30.03	1.05

body and filling material, holing ratio, tensile reinforcement ratio, and volume fraction of the steel mesh, the two proposed equations can be used with confidence to forecast the ultimate load and bending moment capacity of hollow-core ferrocement concrete beams/slabs reinforced with steel meshes. The results of these equations closely match the experimental findings of earlier studies.

Author contributions
YBS and BAE contributed to conceptualization, funding acquisition, investigation, and project administration. SGY contributed to conceptualization, resources, supervision, validation, and writing. SF contributed to conceptualization, funding acquisition, investigation, project administration, resources, supervision, validation, and writing. All the authors read and approved the final manuscript.

Author's information
Yousry B. Shaheen and Boshra A. Eltaly are Professors in the Department of civil engineering, Menoufia University, Shebin ElKoum, Egypt. Shaimaa G. Yousef Msc is a student in the Department of civil engineering, Menoufia University, Shebin ElKoum, Egypt. Sabry Fayed ia an Assistant Professor in the Department of Civil Engineering, Faculty of Engineering, Kafrelsheikh University, Kafrelsheikh, Egypt.

Availability of data and materials
The experimental data can be obtained through email communication with the author at sabry_fayed@eng.kfs.edu.eg.

Declarations

Ethics approval and consent to participate
Not applicable.

Consent for publication
All the authors agree that this article will be published after acceptance.

Informed consent
Informed consent was obtained from all individual participants included in this study.

Competing interests
The authors declare that they have no competing interests.

References

Ababneh, A., Al-Rousan, R., Alhassan, M., & Alqadami, M. (2017). Influence of synthetic fibers on the shear behavior of lightweight concrete beams. *Advances in Structural Engineering, 20*(11), 1671–1683.

Abbass, A. A., Abid, S. R., Arnaot, F. H., Al-Ameri, R. A., & Özakça, M. (2020). Flexural response of hollow high strength concrete beams considering different size reductions. *Structures*. https://doi.org/10.1016/j.istruc.2019.10.001

Abdulhusain, H. M., & Ismael, M. A. (2020). Structural behavior of hollow reinforced concrete beams: A review. *Diyala Journal of Engineering Sciences, 13*(4), 91–101.

Abdullah, Q. N., & Abdull, I. A. (2022). Flexural behavior of hollow self compacted mortar ferrocement beam reinforced by GFRP bars. *Case Studies in Construction Materials*. https://doi.org/10.1016/j.cscm.2022.e01556

Aboul-Anen, B., El-Shafey, A., & El-Shami, M. (2009). Experimental and analytical model of ferrocement slabs. *International Journal of Recent Trends in Engineering, 1*(6), 25–29.

ACI Committee 549, State of the art report on ferrocement, ACI 549–R97, in manual of concrete practice, ACI, Detroit, 1997, pp.26.

ACI Committee 549-IR-93, Guide for the design, construction and repair of ferrocement, ACI 549-IR-88 and IR 93, in manual of concrete practice, American concrete institute, Farmington hills, Michigan, 1988 and 1993, p. 27.

ACI 549.1R-93 & ACI 549–1R-88, A. C. I. Guide for the Design Construction, and Repair of Ferrocement, ACI Committee 549.1R-93; ACI 549–1R-88 and 1R-93, 1997.

AISC (American Institute of Steel Construction). (2010). "Specification for structural steel buildings." AISC 360–10, Chicago.

Aksoylu, C., Yazman, Ş, Özkılıç, Y. O., Gemi, L., & Arslan, M. H. (2020). Experimental analysis of reinforced concrete shear deficient beams with circular web openings strengthened by CFRP composite. *Composite Structures., 249*, 112561.

Alhassan, M., Al-Rousan, R., & Ababneh, A. (2017). Flexural behavior of lightweight concrete beams encompassing various dosages of macro synthetic fibers and steel ratios. *Case Studies in Construction Materials, 7*, 280–293.

Alhassan, M. A., Al-Rousan, R. Z., Amaireh, L. K., & Barfed, M. H. (2018). Nonlinear finite element analysis of BC connections: influence of the column axial load, jacket thickness, and fiber dosage. *Structures*. https://doi.org/10.1016/j.istruc.2018.08.011

Al-Kubaisy, M. A., & Jumaat, M. Z. (2000). Flexural behavior of reinforced concrete slabs with ferrocement tension zone cover. *Construction and Building Materials, 14*(5), 245–252.

Al-Maliki, H. N., Al-Balhawi, A., Alshimmeri, A. J., & Zhang, B. (2021). Structural efficiency of hollow reinforced concrete beams subjected to partial uniformly distributed loading. *Buildings, 11*(9), 391.

Alnuaimi, A. S., Al-Jabri, K. S., & Hago, A. (2008). Comparison between solid and hollow reinforced concrete beams. *Materials and Structures, 41*(2), 269–286.

Al-Rifai, W. N., Ismaeel, N. N., & Riyad, H. (2017). Rehabilitation of damaged reinforced concrete beams. *IOSR Journal of Mechanical and Civil Engineering, 14*, 58–70. https://doi.org/10.9790/1684-1403065870

Al-Rousan, R. (2017). Influence of polypropylene fibers on the flexural behavior of reinforced concrete slabs with different opening shapes and sizes. *Structural Concrete, 18*(6), 986–999.

Al-Rousan, Rajai Z. (2018). "Behavior of macro synthetic fiber concrete beams strengthened with different CFRP composite configurations. *Journal of Building Engineering, 20*, 595–608.

Al-Rousan, R. Z. (2018b). Empirical and NLFEA prediction of bond-slip behavior between DSSF concrete and anchored CFRP composites. *Construction and Building Materials, 169*, 530–542.

Al-Rousan, R. Z. (2018c). Failure analysis of polypropylene fiber reinforced concrete two-way slabs subjected to static and impact load induced by free falling mass. *Latin American Journal of Solids and Structures*. https://doi.org/10.1590/1679-78254895

Al-Rousan, R. Z., Alhassan, M. A., & AlShuqari, E. A. (2018). Behavior of plain concrete beams with DSSF strengthened in flexure with anchored CFRP sheets—effects of DSSF content on the bonding length of CFRP sheets. *Case Studies in Construction Materials, 9*, e00195.

Al-Smadi, Y. M., Al-Huthaifi, N., & Alkhawaldeh, A. A. (2022). The effect of longitudinal hole shape and size on the flexural behavior of RC beams. *Results in Engineering, 16*, 100607.

Arif, M., & Kaushik, S. K. (1999). Mechanical behavior of ferrocement composites: An experimental investigation. *Cement Concrete Composit, 21*, 301–12.

Baraghith, Ahmed T., Mansour, Walid, Behiry, Reda N., & Fayed, Sabry. (2022). Effectiveness of SHCC strips reinforced with glass fiber textile mesh layers for shear strengthening of RC beams: Experimental and numerical assessments. *Construction and Building Materials, 327*, 127036.

Basha, A., Fayed, S., & Mansour, W. (2020). Flexural strengthening of RC one way solid slab with Strain Hardening Cementitious Composites (SHCC). *Advances in Concrete Construction, 9*(5), 511–527.

Chakrawarthi, V., Jesuarulraj, L. R., Avudaiappan, S., Rajendren, D., Amran, M., Guindos, P., Roy, K., Fediuk, R., & Vatin, N. I. (2022). Effect of design parameters on the flexural strength of reinforced concrete sandwich beams. *Crystals, 12*(8), 1021.

Chandralekha, A., & Surendar, M. (2016). Flexural behavior of reinforced concrete beams with ferrocement lost forms. *IJSRD - International Journal for Scientific Research & Development., 4*, 1940–1942.

Concrete Made with Different Types of Crushed Bricks." IOP Conference Series: Materials Science and Engineering. Vol. 584. No. 1. IOP Publishing, 2019.

Dhinesh, N. P., & Satheesh, V. S. (2017). Flexural behavior of hollow square beam. *Int J Sci Eng Appl Sci (IJSEAS), 3*(3), 236–242.

Dotto, J. M. R., De Abreu, A. G., Dal Molin, D. C. C., & Müller, I. L. (2004). Influence of silica fume addition on concrete physical properties and on corrosion behavior of reinforcing bars. *Cement and Concrete Composites, 26*, 31–39.

Elavenil, S., & Chandrasekar, V. (2007). Analysis of reinforced concrete beams strengthened with ferrocement. *International Journal of Applied Engineering Research, 2*(3), 431–440.

El-Wafa, M. A., & Fukuzawa, K. (2010). Flexural behavior of lightweight ferrocement sandwich composite beams. *Journal of Science and Technology*. https://doi.org/10.20428/jst.v15i1.84

Eswaran, K., Sridhar, J., Karunya, N., & Ranee, R. T. A. (2016). "Study on strengthening of predamaged reinforced concrete beam using ferrocement laminates—a review. *International Research Journal of Engineering and Technology (IRJET), 3*, 325–331.

Fahmy, E. H., Shaheen, Y. B., Abdelnaby, A. M., & Abou Zeid, M. N. (2014). Applying the ferrocement concept in construction of concrete beams incorporating reinforced mortar permanent forms. *International Journal of Concrete Structures and Materials, 8*(1), 83–97.

Fayed, S. (2019). Flexural strengthening of defected rc slabs using strain-hardening cementitious composites (SHCC): An experimental work. *Arabian Journal for Science and Engineering, 45*(5), 3731–3742.

Fayed, Sabry, Badr, Ahmed, Basha, Ali, & Mansour, Walid. (2022). Shear behavior of RC pile cap beams strengthened using ultra-high performance concrete reinforced with steel mesh fabric. *Case Studies in Construction Materials, 17*, e01532.

Hago, A. W., Al-Jabri, K. S., Alnuaimi, A. S., Al-Moqbali, H., & Al-Kubaisy, M. A. (2005). Ultimate and service behavior of ferrocement roof slab panels. *Construction and Building Materials, 19*(1), 31–37.

Hassan, N. Z., Ismael, H. M., & Salman, A. M. (2018). Study behavior of hollow reinforced concrete beams. *Int J Curr Eng Technol, 8*(6), 1640–1651.

Kumar, A. (2005). Ferrocement box sections-viable option for floors and roof of multi-story buildings. *Asian J Civil Eng Build Hous, 6*, 569–582.

Kumbhar, U. N., & Jadhav, H. S. (2018). Flexural behaviour of reinforced concrete hollow beam with polypropylene plastic sheet infll. *Int Res J Eng Technol (IRJET), 5*(5), 1517.

Manikandan, S., Dharmar, S., & Robertravi, S. (2015). Experimental study on flexural behavior of reinforced concrete hollow core sandwich beams. *International Journal of Advance Research in Science and Engineering, 4*(01), 937–946.

Mansour, W., & Fayed, S. (2021). Effect of interfacial surface preparation technique on bond characteristics of both NSC-UHPFRC and NSC-NSC composites. *Structures, 29*, 147–166.

Shaheen *et al. Int J Concr Struct Mater*   (2023) 17:21

Page 24 of 24

Naaman, A. E., Al-Shannag, J. (1994). "Ferrocement with fiber reinforced plastic meshes: preliminary investigation." In: Nedwell P, Swamy NR, editors. Proceedings of the fifth international symposium on ferrocement, Manchester, England, September E and FN Spon, London.

Naaman, A. E. (2000). *"Ferrocement and laminated cementitious composites* (p. 372). Techno Press 3000.

Naaman, A. E. (2000b). *Ferrocement and laminated cementitious composites.* Techno Press 3000.

Nahar, T. T., Rahman, Md. M., Haque, Md. R., & Saha, A. K. (2014). "Effect of wire mesh on the strength of R.C.C. beams repaired using ferrocement layers. *International Journal for Research & Development in Technology (IJRDT), 1,* 13–18.

Navid, S. S., Bhalsing, S. S., & Pankaj, B. A. (2013). Tensile strength of ferrocement with respect to specific surface. *Int. J. Eng. Adv. Technol., 3,* 473–475.

Parthiban, N., & Neelamegam, M. (2017). Flexural behavior of reinforced concrete beam with hollow-core in shear section. *Int Res J Eng Technol (IRJET), 4*(4), 2263–2274.

Rajendran, M., & Soundarapandian, N. (2015). Geopolymer ferrocement panels under flexural loading. *Science and Engineering of Composite Materials, 22,* 331–341.

Ramesht, M. H. (1995). Effect of corrosion on flexural behavior of ferrocement in corrosive environment. *J Ferrocement, 27,* 7–18.

Sakthivel, P.B.; Jagannathan, "A. (2012). Fiber reinforced ferrocement—a review study." In proceedings of the 2nd international conference on advances in mechanical, manufacturing and building sciences (ICAMB-2012), Vellore, India, 9–11 January; pp. 1172–1177

Shaaban, I. G. (2002). "Expanded wire fabric permanent formwork for improving flexural behaviour of reinforced concrete beams," composite materials in concrete construction: proceedings of the international seminar held at the University of Dundee, Scotland, UK, 5–6September, pp. 59–70. https://doi.org/10.1680/cmicc.31746.0006

Shaaban, I. G., Shaheen, Y. B., Elsayed, E. L., Kamal, O. A., & Adesina, P. A. (2018a). Flexural Characteristics of lightweight ferrocement beams with various types of core materials and mesh reinforcement. *Construction and Building Materials, 171*(20), 802–816. https://doi.org/10.1016/j.conbuildmat.2018.03.167

Shaaban, I. G., Shaheen, Y. B., Elsayed, E. L., Kamal, O. A., & Adesina, P. A. (2018b). Flexural behaviour and theoretical prediction of lightweight ferrocement composite beams. *Case Studies in Construction Materials.* https://doi.org/10.1016/j.cscm.2018.e00204

Shah, S., Balaguru, P., & Ferrocement, P. N. (1984). *New reinforced concrete* (pp. 5–24). Blackie and Sons Limited.

Yousry B I Shaheen, Noha M Soliman, and Fathya El-Araby. (2018b). "Repairing reinforced concrete beams with openings by ferrocement laminates", the 12th international conference on civil and architecture engineering ICCAE-12, 3–5 April 2018b. Military Technical College, Kobryn El-Kobbah, Cairo, Egypt.

Shaheen, Y. B., Fatma, M. E., and Manar A. S. D. (2020a). Developing of light weight ferrocement composite plates. Publication https://www.researchgate.net/publication/33869776010. Accessed 17–19 Dec 2019".

Shaheen, Y. B. I., Eltaly, B., & Abdul-Fataha, S. (2014). Structural performance of ferrocement beams reinforced with composite materials. *Structural Engineering and Mechanics, 50*(6), 817–834.

Shaheen, Y. B. I., & Eltehawy, E. A. (2017). Structural behavior of ferrocement channels slabs for low cost housing. *Challenge Journal of Concrete Research Letters., 8*(2), 48–64.

Shaheen, Y. B. I., Etman, Z. A., & Ramadan, A. G. (2018a). Characteristics of ferrocement lightweight wall. *International Journal of Civil Engineering, 16*(1), 33–45.

Shaheen, Y. B. I., Mousa, M., & Gamal, E. E. (2020). Structural behavior of light weight ferrocement walls. *IOP Conference Series: Materials Science and Engineering, 974*(1), 012037.

Shaheen, Y. B. I., Etman, Z., & Elrefy, A. M. (2022). Structural behavior of ferrocement composite hollow-cored panels for roof construction. *Challenge Journal of Concrete Research Letters, 13*(1), 5–27.

Syahrul, S., Tjaronge, M. W., Djamaluddin, R., & Amiruddin, A. A. (2021). Flexural behavior of normal and lightweight concrete composite beams. *Civil Engineering Journal, 7*(3), 549–559.

Thenmozhi, S. D. S. R., & Shri, S. D. (2012). An Experimental investigation on the flexural behavior of scc ferrocement slabs incorporating fibers. *International Journal of Engineering Science and Technology (IJEST), 4,* 2146.

Thiyab, H. M. (2016). Experimental study of reinforced light weight concrete beams. *Journal of University of Babylon, 24*(4), 1086–1098.

Torri, K., & Kawamura, M. (1990). Chloride induced corrosion of steel reinforcement made with various mineral admixtures. *Trans Jpn Conc Inst, 12,* 183–190.

Varghese, N., & Joy, A. (2016). Flexural behavior of reinforced concrete beam with hollow core at various depth. *Int J Sci Res (IJSR), 5*(5), 741–746.

Varma, M. B., & Hajare, M. B. (2015). Ferrocement: Composite material and its applications. *Int J Pure Appl Res Eng Technol, 3,* 296–307.

Vicridge, I.G.; Ranjabar, M.M. (1998a). "The effect of aggressive environment on the flexural performance of ferreocement." In proceedings of the 6th international symposium on ferrocement, Ann Arbor, MI, USA, 7–10 June; pp. 313–328.

Vickridge, I.G.; Ranjbar, M.M. (1998b). "The combined effect of crack, load and aggressive environment on the corrosion rate of ferrocement reinforcement." In proceedings of the 6th international symposium on ferrocement, Ann Arbor, MI, USA, 7–10 June; pp. 329–343.

Wang, S., Naaman, A. E., & Li, V. C. (2004). Bending response of hybrid ferrocement plates with meshes and fibers. *J Ferrocement, 34*(1), 275–288.

Publisher's Note